energies

MDPI

Article

Power Quality Improvement in HRES Grid Connected System with FOPID Based Atom Search Optimization Technique

Ch. Rami Reddy [1,*], B. Srikanth Goud [2,*], Flah Aymen [3], Gundala Srinivasa Rao [4] and Edson C. Bortoni [5]

[1] Department of Electrical and Electronics Engineering, Malla Reddy Engineering College (A), Maisammaguda, Secunderabad 500100, Telangana, India
[2] Department of Electrical and Electronics Engineering, Anurag College of Engineering, Ghatkesar 501301, Telangana, India
[3] Research Unit of Energy Processes Environment and Electrical Systems, National Engineering School of Gabes, University of Gabes, Gabes 6029, Tunisia; flahaymening@yahoo.fr
[4] Department of Electrical and Electronics Engineering, CMR College of Engineering & Technology, Hyderabad 501401, Telangana, India; drgundalasrinivasarao@gmail.com
[5] Electric and Energy Systems Institute, Itajubá Federal University, Itajubá 37500, Brazil; bortoni@unifei.edu.br
* Correspondence: crreddy229@gmail.com (C.R.R.); srikanth.b@anuraghyd.ac.in (B.S.G.); Tel.: +91-9030937167 (B.S.G.)

Abstract: An intelligent control strategy is proposed in this paper which suggests the Optimum Power Quality Enhancement (OPQE) of grid-connected hybrid power systems with solar photovoltaic, wind turbines, and battery storage. Unified Power Quality Conditioner with Active and Reactive power (UPQC-PQ) is designed with Atom Search Optimization (ASO) based Fractional-order Proportional Integral Derivative (FOPID) controller in the proposed Hybrid Renewable Energy Sources (HRES) system. The main aim is to regulate voltage while reducing power loss and reducing Total Harmonic Distortion (THD). UPQC-PQ is used to mitigate the Power Quality (PQ) problems such as sag, swell, interruptions, real power, reactive power and THD reductions related to voltage/current by using ASO based FOPID controller. The developed technique is demonstrated in various modes: simultaneous to improve PQ reinforcement and RES power injection, PRES > 0, PRES = 0. The results are then compared to those obtained using previous literature methods such as PI controller, GSA, BBO, GWO, ESA, RFA, and GA and found the proposed approach is efficient. The MATLAB/Simulink work framework is used to create the model.

Keywords: PV; wind; BESS; UPQC-PQ; sag; swell; disturbances; total harmonic distortion

Citation: Reddy, C.R.; Goud, B.S.; Aymen, F.; Rao, G.S.; Bortoni, E.C. Power Quality Improvement in HRES Grid Connected System with FOPID Based Atom Search Optimization Technique. *Energies* **2021**, *14*, 5812. https://doi.org/10.3390/en14185812

Academic Editors: Victor Fernao Pires and Georgios Christoforidis

Received: 29 July 2021
Accepted: 9 September 2021
Published: 14 September 2021

1. Introduction

Renewable Energy Sources (RES) based Distribution Generation (DG) is gaining a prominent role nowadays with the technological development, environmental concerns and huge demand for electricity to the utility grid. RESs will reduce pollution and global warming while also providing substantial economic benefits. RESs-based distributed generation (DG) is becoming more important as a result of global economic challenges and the ecological consciousness [1]. Many RESs, such as wind energy, photovoltaic energy, fuel cells (FCs), and biomass, have been introduced and incorporated into traditional power networks [2]. In terms of being AC or DC, each RES has distinct characteristics that set it apart from other sources. PV and FC generated DC voltages of varying ranges, while wind energy produces either AC or DC depending on the generator used in the wind energy conversion system (WECSs) [3]. These variations render linking these RESs to the electrical grid challenging. Another issue that arises when incorporating these RESs into the electrical grid is the power produced from them becoming unstable due to their reliance on changing environmental factors, such as temperature and irradiance in PV systems and wind speed in WECSs. The use of power electronic equipment to change the DClevels of all

DC sources using certain converters is a vital solution to such problems. These converters can also be used to maximize the amount of power produced from each RES [4].

The output of these RESs is then connected to the electrical grid using DC-AC inverters. The power electronic devices used to connect various forms of renewable energy sources to the grid would exacerbate PQ issues such as voltage sags/swells, disturbance harmonics, and so on. If grid requirements or codes are not met, these issues can result in continuous fluctuations in power produced and tripping of some RESs [5]. Flexible AC Transmission Systems (FACTS) devices [6] are modular devices that can be attached to the whole system to support the PQ and increase system performance. There are three types of network interfaces for FACTS devices: series, parallel, and a mixture of series and parallel. Until being incorporated into the scheme, each of these three categories has its own set of characteristics and uses that must be defined and regulated. The transmission line cap is increased and the line reactance is changed using Series FACTS equipment. Static Synchronous Series Compensator (SSSC) and Dynamic Voltage Restorer (DVR) are two of them, as seen in [7]. During voltage sag/swell conditions, shunt forms are used to sustain the voltage by sharing reactive power with the device. To boost the relation of certain RESs to the grid, shunt compensators such as Static compensators (STATCOM), Distribution STATACOM (DSTATCOM), and Thyristor Controlled Reactor (TCR) were implemented [7].

These FACTS devices' series/shunt hybrid merged the characteristics of series and shunt devices like centralized Power flow controller (UPFC) and distributed power flow controller (DPFC) [8]. UPFC is a device that combines STATCOM and SSSC through a DC connection to exchange active/reactive data with the system. By removing the DC connection capacitor and connecting STACOM and SSSC through a transmission line with third frequency components, certain changes to the configuration of the UPFC are made. Since the DC connection has been eliminated, the STATCOM and SSSC will now be mounted separately. According to the preceding discussions, certain FACTS devices are needed to address the PQ issues in grid-connected hybrid RESs (HRESs). The controller used defines the output of the various types of FACTS instruments. Traditional PI controllers and modified fractional-order PI controllers (FOPI) are the most common due to their ease of use and high accuracy, with the FOPI model having the edge [9]. Adjusting or Tuning the FOPI controller parameters in FACTS devices to minimize PQ problems in grid-connected HRESs is a non-linear complex optimization problem that necessitates the use of metaheuristics optimization techniques. In several HRESs implementations, many optimization strategies for optimum tuning of PI and FOPID controller parameters have been introduced. This paper majorly focuses on compensating various PQ issues like sag, swell, disturbances, nonlinear and unbalance load conditions in the HRES interfaced grid connected system. The proper control scheme and Truth unit were certainly chosen to mitigate the system's PQ concerns.

Main Contribution and Organization of the Paper

This paper mainly focuses on the mitigation of PQ problems in HRES systems due to voltage/current related issues, sag, swell, disturbances, non-linear load, unbalance load and THD reduction. The proposed ASO based FOPID controller with UPQC-PQ device which is effectively used to mitigate these problems. The main contribution of the paper is presented as follows:

- RES is designed with PV, wind and battery as an energy storing device and can be utilized when the sources are absent. BESS is used to store the excess energy generated from the sources and can be utilized to meet the required demand under critical environmental conditions.
- RES is connected to the grid system and at the PCC a non-linear load, unbalanced load or both may be connected. The integrated system may introduce harmonics and unbalances under distorted supply voltages. This affects the stability and reliability of the system which can be overcome by the utilization of ASO based FOPID controller.

- The proposed control strategy is designed and validated by connecting non-linear load and unbalanced loads at the PCC.

The remaining portion of the paper is organized as follows: Section 2 revises the relevant works on PQ mitigation. Section 3 includes a description of the proposed system architecture. The mathematical simulation of RES components in the proposed design is discussed in this section, as well as a comprehensive overview of the UPQC-PQ. In Section 4, the proposed architecture with a control structure is defined in detail. In Section 5, the FOPID controller is defined, as well as how to use the optimization algorithm. A detailed overview of ASO is provided in Section 6, along with updating functions. In Section 7, the suggested method's findings and debates are evaluated and checked. Finally, Section 7 brings the article to a close.

2. Recent Research Works: A Brief Review

In practice, there are several methods to compensate for the PQ problems with various custom power devices (Table 1). This section describes few methods related to mitigating PQ problems.

Table 1. Brief review of previously published work.

Proposed Methodologies	Year	Reference
• They proposed modelling, control and design analysis of single-stage, three-phase renewable energy sources based on DG where the inverters are controlled to perform multi-functions using an active power filter. • To improve the power quality at PCC without affecting its normal operation of real power transfer they proposed a novel control strategy with a DG and grid interface inverter.	2013	[10]
• They proposed a hybrid renewable energy system consists of PV, Wind and mini-hydro system • They have explored how to improve load voltage, current and mitigating harmonics using a Static compensator	2015	[11]
• They proposed distributed control strategy in DC microgrids and obtaining large-signal stability • To maintain the load power constant they introduced a feedback controller which is proposed to stabilize the system.	2016	[12]
• They presented optimal sizing of PV based UPQC-DG by power angle control • They provided an optimum sizing technique for UPQC-DG which reduces reactive power disturbance using shunt and series converters	2018	[13]
• They proposed PV fed UPQC for Power quality improvement • JAYA Algorithm was proposed which mainly consists of two objective functions used in shunt and series inverter control of PV-UPQC for the improvement in voltage and control at various operational conditions.	2018	[14]
• They proposed a hybrid renewable energy system consists of PV, Wind and Fuel cells for enhancing the PQ using the HIL testing platform. • They proposed a Synchronous reference frame theory-based shunt active power filter to mitigate the current harmonics in the source current • The control strategy is based on ANFIS which is validated through HIL with the help of OPAL-RT hardware controller	2019	[15]
• They proposed a microgrid integrated with PV, Wind and BESS. • They implemented a modified version of the adaptive filtering technique with Momentum based Least Mean Square control technique which is used to provide the control signal to grid side voltage source converter	2019	[16]
• They proposed grid connected wind system and Battery as energy storage that can be utilized in the absence of wind. • They have addressed various power quality issues and mitigation using DSTATCOM with BESS	2019	[17]

Table 1. *Cont.*

Proposed Methodologies	Year	Reference
• They presented UPQC strategy for power quality improvement based on dq0 detection method • The fundamental and harmonic detection on the power supply side current and load side voltage are performed with the help of Space Vector Pulse width Modulation (SVPWM)	2020	[18]
• They have presented Fuzzy Logic controller (FLC) based UPQC in the distribution system for enhancing the concern of the power quality. • UPQC was outlined by combining a series of APF and shunt APF. The adaptable FLC is composed of the series APF control of voltage distortion • The operation of Shunt APF was controlled by d−q axes current from load current and DC-interface voltage was maintained through adaptable FLC.	2020	[19]

Some of the commonly identified problems:

- In static VAR compensator voltage regulations were not done properly
- Series APF were only used for low power applications
- Conduction losses are higher when multi level converters are utilized

In the recent decade, the usage of renewable energy sources is emerging, it has many advantages. But while the integration of renewable source to the electric grid it will create some power quality issues. So, in the pieces of literature, many techniques have been proposed, but the problem is not yet completely solved. Hence in this paper, an optimization-based control strategy is proposed to enhance the power quality while the integration of renewable energy sources.

3. Proposed HRES System Model with Description

The utilities also changed as a result of the increased load demand in the grid as a result of the urbanization and industrialization process in real-time standards [20]. In the recent modern power grid, traditional generation sources are insufficient to satisfy the necessary power demand, resulting in increased protection and power reliability concerns [21]. In recent decades, traditional generation technologies have released a significant amount of contaminants, which have been described as major concerns. Distributed and green energy sources are used to minimize emissions to produce a significant volume of energy to substitute for load demand on the utility side and offset these issues in the grid [22]. The HRES system is the most sophisticated system, capable of increasing the system's performance and reliability. The HRES can be paired with a delivery system to satisfy necessary load demand from the customer side, but this poses a problem of power quality reliability and versatility. Power quality problems occur as a result of HRES adaptation in a grid-connected environment and must be minimized to ensure the system's reliability and flexibility. The Reality gadget is one of the most popular solutions for voltage sag, sale, interference, disruption, and other PQ issues. UPQC-PQ (real and reactive power) is thus implemented in the HRES in this paper to compensate for power quality issues such as voltage swell, voltage sag, voltage interference, and voltage disruptions. With the support of the UPQC-PQ system, PQ problems are reduced. The UPQC-PQ system gets its name from the fact that it deals with actual and reactive power control theory. The HRES is made up of PV panels and a wind turbine that is attached to the grid. The battery is built with HRES to satisfy load demand and under critical environmental conditions of PV and Wind. PQ problems are rising due to nonlinear load, unbalanced loads when connected to grid interfaced HRES system [16]. This leads to a reactive power mismatch issue and increased voltage instability.

As a result, to ensure reliable service, power quality problems must be minimized, which is achieved with the aid of UPQC-PQ. The UPQC-PQ could be the best instrument for improving voltage control in grid-interfaced HRES while still resolving power quality issues. With the production of the FOPID controller, the proper management of UPQC-PQ

is strengthened. With the aid of ASO, the controller makes the most possible improvement. Figure 1 illustrates a block diagram of the proposed procedure. HRES are used to meet the global load requirements. Excess power produced by the PV and WT is stored in the battery and can be utilized during critical conditions when required. The power quality challenges of the grid-connected HRES system are a major challenge in ensuring stability and efficiency. On the grid side, fault conditions, non-linear load, and critical load lead to PQ issues in the HRES. Power quality problems must be overcome in a grid-interfaced HRES system to work efficiently. The UPQC-PQ is equipped with HRES interfaced grid-connected system that compensates for sag, swell, nonlinear, unbalance loads and disturbance in the PQ. The UPQC-PQ uses series and shunt filer control methods to compensate for PQ problems. Filters are given the best gain parameters for injecting necessary power to compensate PQ issues using the FOPID controller whose parameters can be calibrated with ASO, which is used to choose the right values for low-power control operation.

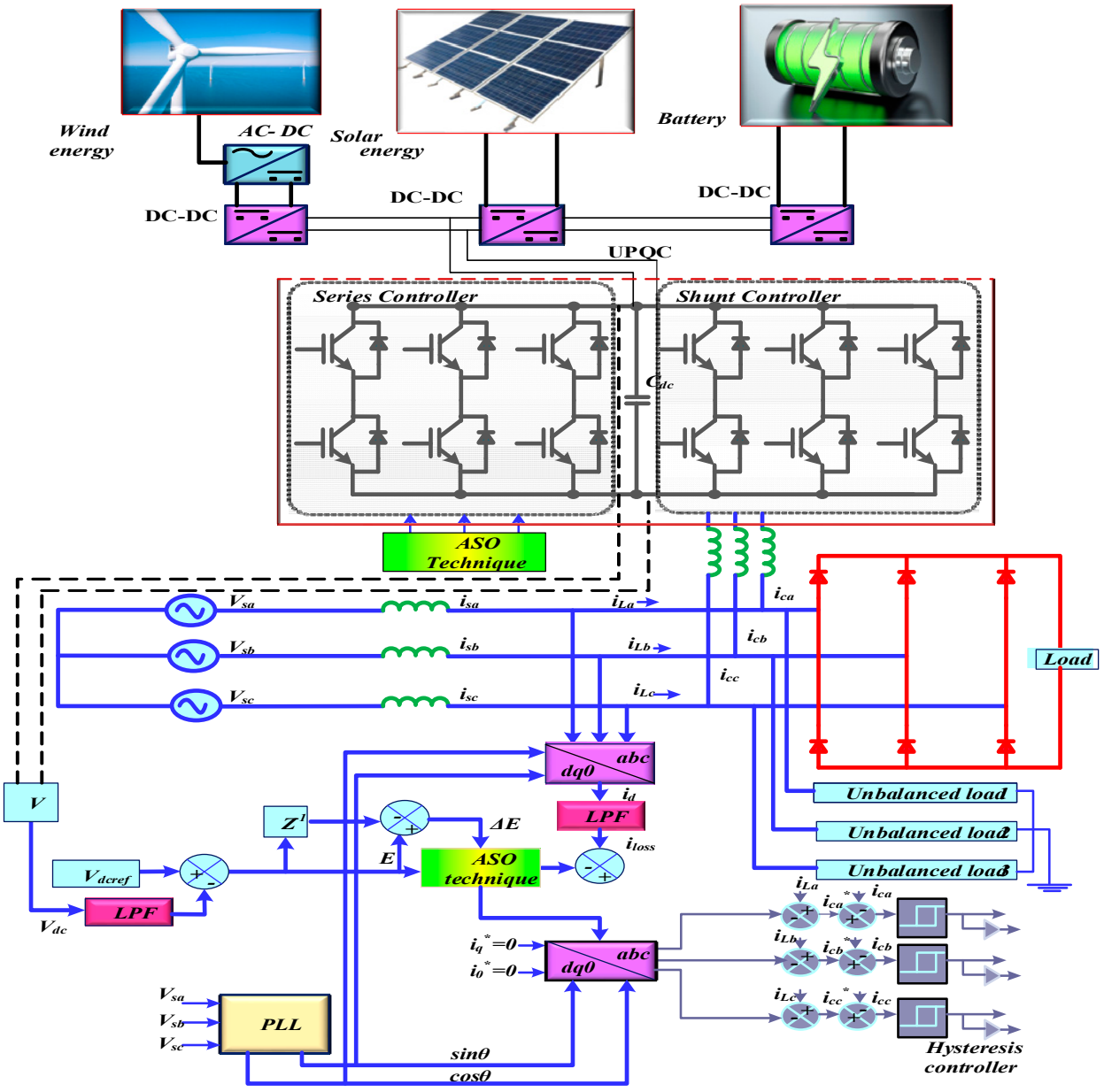

Figure 1. Block diagram of the Proposed System.

3.1. Modeling of PV

PV is the best alternative option for generating electricity from solar energy without releasing greenhouse gases, durability with non-rotating units, long lifespan, good efficiency, and low maintenance, among the numerous renewable resources. To achieve the appropriate voltage, the PV system consists of cells connected in series [17]. The PV plane of the final output voltage is calculated by multiplying the terminal voltage by the output current. The PV panel's built model is depicted in Figure 2.

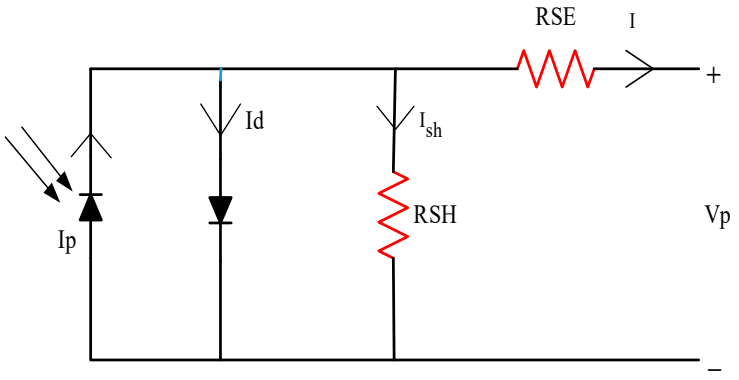

Figure 2. Equivalent circuit of PV.

The design PV panel current and terminal voltage is computed based on the Equations (1) and (2),

$$I_P = I_{SC} - I_0\left\{\exp\left[\frac{Q}{akt}(V_P + I_P R_{SE}) - 1\right]\right\} - \frac{V_P + I_{SC}R_{SE}}{R_{SH}} \quad (1)$$

$$V_P = \frac{akt}{Q}\ln\left\{\frac{I_{SC}}{I_P} + 1\right\} \quad (2)$$

where Q is the electron charge, k is the Boltzmann's constant and is the diode ideality component, t is the temperature in Kelvin, R_{SE} is the series resistance, R_{SH} is the shunt resistance, I_{SC} is the current, and V_P is the cell voltage. The PV panel's generated power is calculated as (3)

$$P_{PV}(t) = N_{pv}(t) \times I_{pv}(t) \times V_{pv}(t) \quad (3)$$

where P_{PV} is the power of PV, $N_{PV}(t)$ is the number of cells in the PV array, $I_{PV}(t)$ is the current of PV and $V_{PV}(t)$ is the voltage of PV. Extracting maximum power from the grid is not happens at all times related to available current and load. To extract the maximum power of PV under load conditions, maximum power point tracking is normally used. Various types of methods are available, in this proposed method perturb and observer method is used.

3.2. Modelling of WT

The output power was provided by the wind turbine based on wind speed at a certain hub height [18]. The wind speed is related to the following Equation (4), based on the wind turbine,

$$P_W T(t) = \begin{cases} 0, V < V_{cutin} \text{ or } V > V_{cutout} \\ P_{WT}^{MAX}\left(\frac{P_{WT}^{CO} - P_{WT}^{MAX}}{V_{cutout} - V_r}\right)(V(t) - V_r \quad), V_r < V \le V_{cutout} \\ P_{WT}^{MAX}\left(\frac{V(t) - V_{cutin}}{V_r - V_{cutin}}\right)^3, V_{cutin} \le V \le V_r \end{cases} \quad (4)$$

where P_{WT}^{CO} represents wind turbine power at cutout voltage, $V(t)$ represents wind speed at time t, V_r represents nominal wind speed, V_{cutout} represents wind turbine cutout speed,

V_{cutin} represents wind turbine cut-in speed, and P_{WT}^{MAX} represents wind turbine maximum power. On the grid side, PV and wind turbine systems are used to balance load demand. As load demand exceeds HRES's ability to compensate, a battery is also attached to the device. The battery system's statistical modelling is presented in the section below.

3.3. Modelling of BESS

When the power produced by the HRES is insufficient, the battery supplies to load demand. In the case of the system's necessary power demand, the capacity of the battery was computed and considered using the reference autonomy day (AD) shown below Equation (5).

$$B^{capacity} = \frac{Autonomyday \times P^L}{\eta^I \times \eta^B \times DOD} \tag{5}$$

where *DOD* stands for the battery's depth of discharge rate, η^B known as the battery's efficiency, η^I stands for inverter efficiency and P^L stands for demand strength. The average number of days that a battery will supply power to compensate for load demand is referred to as AD [19]. The battery is used to store the excess power produced by the RES. The battery capacity is calculated using Equation (6).

$$B^P = P_{PV}(t) + P_{WT}(t) - \frac{P_L(t)}{\eta^I} \tag{6}$$

where $P_L(t)$ is the system's load demand and B^P what is the battery capacity. State of Charge (SOC) is a critical parameter in the battery that is related to extra energy production and energy deficiency in HRES, as seen in (7).

$$SOC = \begin{cases} SOC(t-1)(1-\mu) + \left(P_{PV}(t) + P_{wT}(t) - \frac{P_L(t)}{\eta^t}\right) \times \eta^B, P_{PV}(t) + P_{wT}(t) > P_L(t) \\ SOC(t-1)(1-\mu) + \left(\frac{P_L(t)}{\eta^I} - P_{PV}(t) + P_{wT}(t)\right) \times \eta^B, P_{PV}(t) + P_{wT}(t) < P_L(t) \end{cases} \tag{7}$$

where μ is the self-discharge rate of the battery. PQ such as sag, swell, voltage interference, and so on can affect the proposed design method. The power quality problems in the system must be resolved to improve the system's reliability, which was achieved by the use of the UPQC-PQ unit in the HRES system. The UPQC-PQ modelling is presented in the section below.

3.4. Modelling of UPQC

Enhancing the power efficiency in the power grid is a critical solution that can be done with the aid of power electronic-based power conditioning appliances. In this article, a UPQC-PQ solution is chosen to compensate for power quality problems in the HRES framework. This device will compensate for PQ issues. To compensate for power quality problems in the system, a range of FACT devices are available. Similarly, the UPQC-PQ can be used to alleviate voltage and current PQ problems. Sag, swell, unbalance, flickers, and harmonics are all PQ problems. In general, the UPQC-PQ uses two forms of Voltage Source Inverters (VSI): shunt and series Active Power Filter (APF), as well as a DC connection capacitor [20]. The key factor that regulates the voltage between two filters is the DC-link capacitor. The UPQC-configuration is represented in Figure 3.

The vector diagram of the UPQC-PQ with over-voltage compensation is illustrated in Figure 4b. The general mathematical model of UPQC-PQ is presented in this section. The power system with the UPQC-PQ device can be divided into different units such as generation with power supply system, series, and shunt active filters. The power supply system is mathematically modelled with Kirchhoff's law which is presented in (8) and (9),

$$V^{if} = e^i - L^s \frac{di_s}{dt} - R^s I^{is} - V^{ih} \tag{8}$$

$$I^{is} = I^{iL} - I^{ih} \tag{9}$$

where I^{ih} is described as output current of shunt active filter, I^{iL} is described as load current, I^{is} is described as line current, V^{ih} is described as the output voltage of series active filter, e^{i} is described as source voltage, L^{S} is described as the inductance of the transmission line, R^{s} is described as the resistance of the transmission line, i in the subscript is described as a, b and c phases in the power system illustrated in Figure 4a. The equivalent circuit of the UPQC-PQ is illustrated in Figure 4b. The source current and load voltage are regulated by a series and shunt active filter in this UPQC-PQ system. The series and shunt active filters provide necessary voltage and current when power quality problems arise in the power system [21,22]. $I(ch)$ and $I(s)$ are often used to reflect load and source currents, respectively. $I(f)$ reflects the injected current of a shunt active power filter, and $V(c)$ represents the injected voltage of a series active power filter. The injected voltage of a series active filter, denoted by $V(ch)$, is used as the reference load voltage. The load's power factor is defined as $cos\phi(n)$ and the source voltage factor fluctuation is described as k. Equation (10) shows the difference of sources voltage to reference voltage to the ratio of the reference voltage. The vector diagram of the UPQC-PQ is illustrated in Figure 4c which denotes the voltage compensation. When over-voltage V'_G has occurred in the system then the series inverter injects the negative voltage $V'_{seriesinverter}$ into the grid to eliminate it.

$$V(c) = V(ch) - V(s) = -kV(ch) < 0^{0} \tag{10}$$

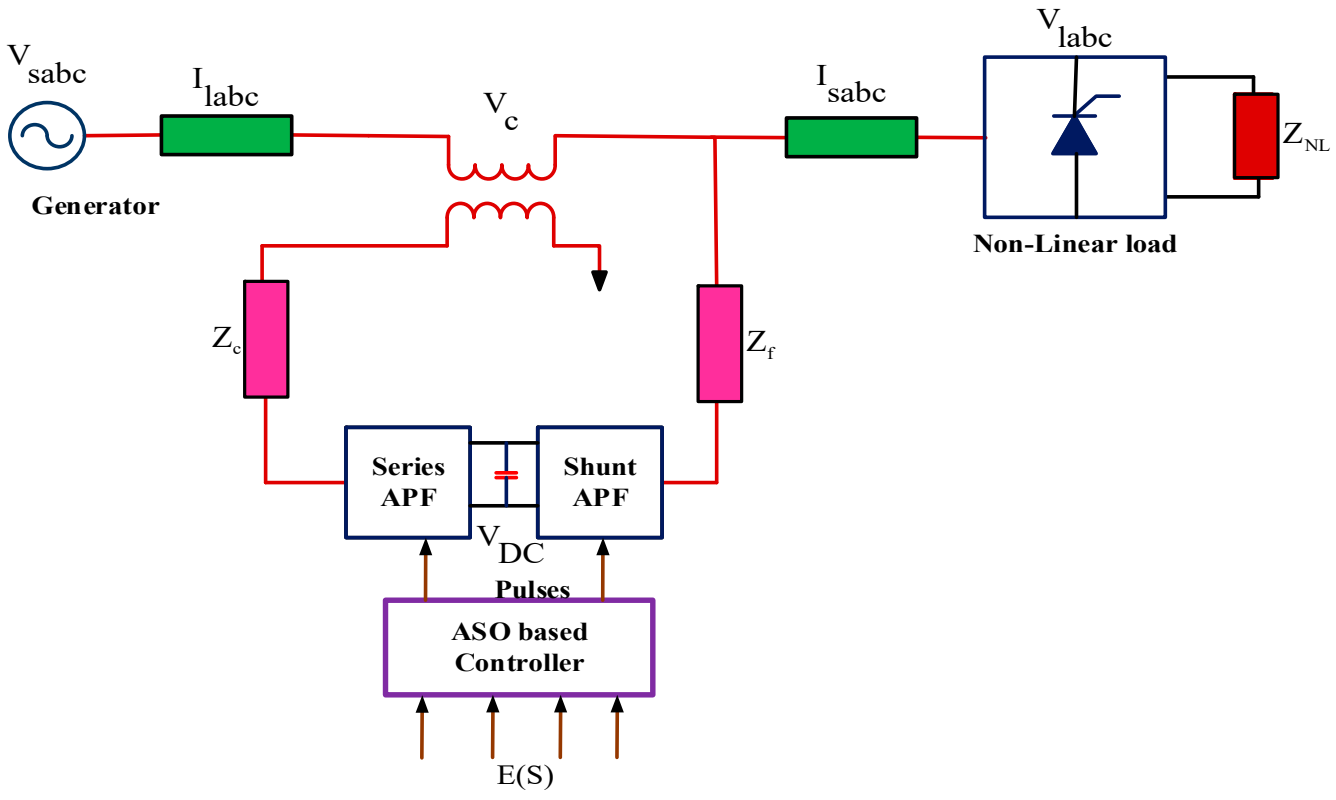

Figure 3. Structural model of UPQC.

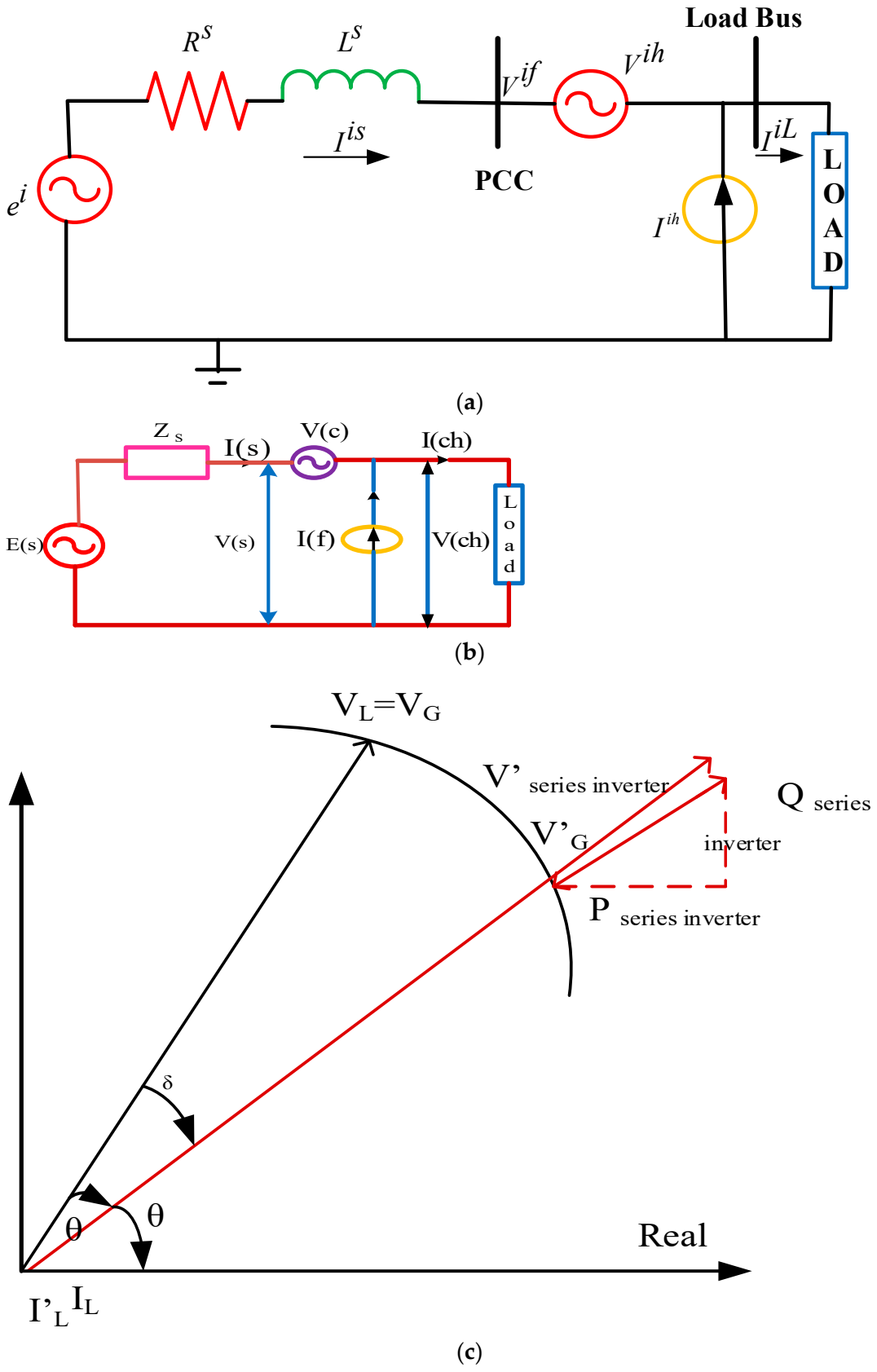

Figure 4. Analysis of (**a**) Equivalent circuit (**b**) Equivalent circuit model of UPQC and (**c**) Vector diagram of voltage compensation.

The above equation can be solved by using Equation (11)

$$k = \frac{V(s) - V(ch)}{V(ch)} \tag{11}$$

In UPQC-PQ designs, the losses are omitted. The power requirement of active power and load are considered equal to PCC input. The PCC side current is described as below Equation (12)

$$I(f) = \frac{I(ch)}{1+k} \cos\phi(n) \tag{12}$$

In the UPQC, series and shunt active power filter apparent power is formulated as (13) and (14),

$$A(c) = P(c) + jQ(c) \tag{13}$$

$$A(f) = V(ch)I(f) \tag{14}$$

where $Q(c) = V(c)I(s)$; $Q(c) = V(c)I(s)\cos\phi(s)$, $P(c)$ is described as the active power of series filter and $Q(c)$ is described as reactive power of series filter, The difference among input load current as well as the source current with the load harmonics current as well as the reactive current is described as $I(f)$. In the UPQC-PQ device, the series and shunt active power filter is controlled with ASO based FOPID controller. Then the controller is used to improve the stability of the system by compensating power quality issues.

4. Control Strategy

The load demand of the delivery system has risen in recent years as a result of modern industrialization and urbanization. The HRES is selected to satisfy electricity load needs in the delivery grid while avoiding pollution issues. The HRES provides the necessary power while avoiding unwanted carbon emissions and global warming issues. The HRES dilemma is applied to grid-connected networks, posing a problem with reliability and power efficiency. The issue of power efficiency is a crucial one that must be resolved for the system's reliability and versatility to be sustained. With the support of the UPQC-PQ system, power quality issues must be resolved. The implementation of a proper control strategy in the framework increases the performance of the UPQC-PQ computer. With UPQC-PQ and the proposed controller, the proper power efficiency enhancement of HRES with a grid connection is accomplished. In the HRES method, the suggested controller operates in combination with the FOPID controller and ASO. The UPQC-PQ control has two controllers: series APF and shunt APF. In the HRES method, control methods are used to fix power quality problems. The following section provides a more detailed overview of the sequence as well as the shunt active power filter. This section includes a detailed summary of both series and shunt active power filters.

4.1. Control Strategy of Series Active Power Filter

Figure 5 depicts the series active power filter-based control mechanism. Initially, we measure the reference voltage at first. After the three-phase voltage is measured, it is converted into d-q axes using the dq transformation method (Clarke transformation) [23]. In this method, power filters are often used to monitor the UPQC-PQ to address power quality issues in the system [24]. Equation (1) shows the mathematical representation of the dq transition mechanism from the three-phase voltage (15),

$$\begin{bmatrix} V^0 \\ V^d \\ V^q \end{bmatrix} = \frac{2}{3} \begin{bmatrix} \frac{1}{2} & \frac{1}{2} & \frac{1}{2} \\ \sin(\alpha t) & \sin\left(\alpha t - \frac{2\pi}{3}\right) & \sin\left(\alpha t + \frac{2\pi}{3}\right) \\ \cos(\alpha t) & \cos\left(\alpha t - \frac{2\pi}{3}\right) & \cos\left(\alpha t + \frac{2\pi}{3}\right) \end{bmatrix} \begin{bmatrix} V^a \\ V^b \\ V^c \end{bmatrix} \tag{15}$$

where V^d is described as direct axes voltage, V^q is described as quadrature axes voltage, V^a, V^b and V^c is described as three-phase voltages.

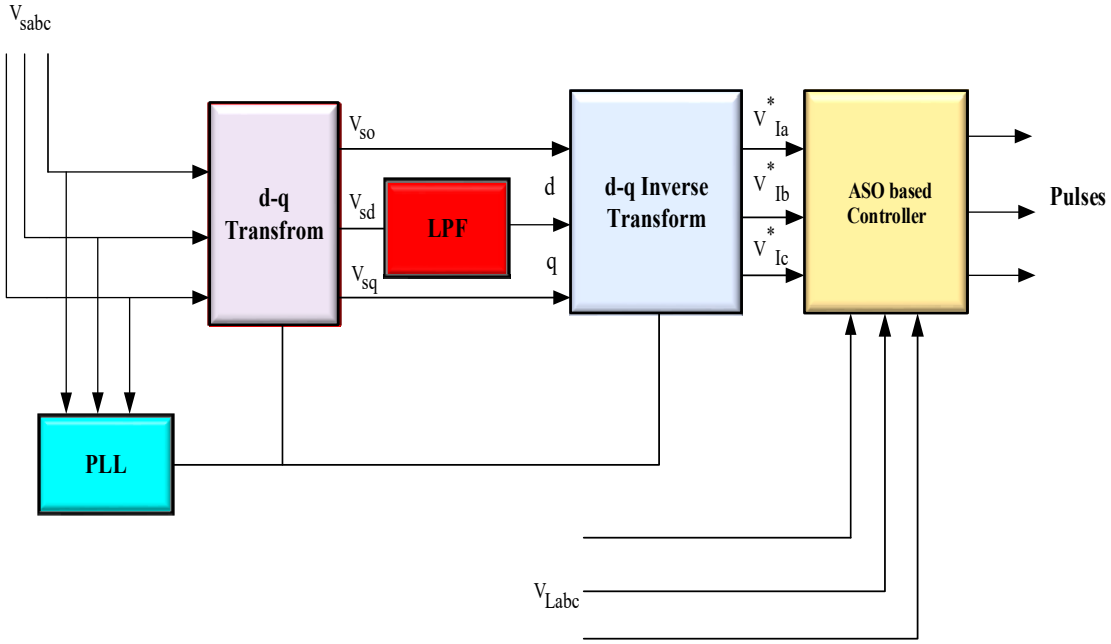

Figure 5. Block diagram of Series APF.

The *d* axis voltage is represented as a direct voltage as well as the alternating component voltage. The d axis voltage can be smoothing by the Low Pass Filter (LPF) which is mathematically formulated as (16)

$$V^{d(dc)} = V^{d} - V^{d(ac)} \tag{16}$$

where $V^{d(ac)}$ is considered as ac component voltage and $V^{d(dc)}$ is considered as dc component voltage. After that, the voltage is changed into three phases as (17)

$$\begin{bmatrix} V^{Ra} \\ V^{Rb} \\ V^{Rc} \end{bmatrix} = \frac{2}{3}\begin{bmatrix} \sin(\alpha t) & \frac{1}{2} & 1 \\ \sin(\alpha t) & \sin\left(\alpha t - \frac{2\pi}{3}\right) & 1 \\ \cos(\alpha t) & \cos\left(\alpha t - \frac{2\pi}{3}\right) & 1 \end{bmatrix}\begin{bmatrix} V^{d(dc)} \\ V^{q} \\ V^{o} \end{bmatrix} \tag{17}$$

where, V^{Ra}, V^{Rb}, V^{Rc} is denoted as the three-phase reference voltages. The hysteresis band of the voltage is controlled using the control pulses which are calculated and tuned by FOPID with ASO. Similarly, the shunt active power filter with a control algorithm is presented in the following section.

4.2. Control Strategy of Shunt Active Power Filter

The shunt active power filter control strategy with the proposed controller is illustrated in Figure 6. The three-phase currents and voltages are changed into α and β which are described in the following Equations (18) and (19) [25],

$$\begin{bmatrix} V^{s0} \\ V^{s\alpha} \\ V^{s\beta} \end{bmatrix} = \sqrt{\frac{2}{3}}\begin{bmatrix} \frac{1}{\sqrt{2}} & \frac{1}{\sqrt{2}} & \frac{1}{\sqrt{2}} \\ 1 & -\frac{1}{2} & -\frac{1}{2} \\ 0 & \frac{\sqrt{3}}{2} & -\frac{\sqrt{3}}{2} \end{bmatrix}\begin{bmatrix} V^{sa} \\ V^{sb} \\ V^{sc} \end{bmatrix} \tag{18}$$

$$\begin{bmatrix} I^{l0} \\ I^{l\alpha} \\ I^{l\beta} \end{bmatrix} = \sqrt{\frac{2}{3}}\begin{bmatrix} \frac{1}{\sqrt{2}} & \frac{1}{\sqrt{2}} & \frac{1}{\sqrt{2}} \\ 1 & -\frac{1}{2} & -\frac{1}{2} \\ 0 & \frac{\sqrt{3}}{2} & -\frac{\sqrt{3}}{2} \end{bmatrix}\begin{bmatrix} I^{La} \\ I^{Lb} \\ I^{Lc} \end{bmatrix} \tag{19}$$

where, $I^{l\alpha}$, $I^{l\beta}$ is considered as phase neutral currents, I^{La}, I^{Lb}, I^{Lc} is described as three-phase load currents $V^{s\alpha}$ $V^{s\beta}$ is considered as phase neutral voltages and V^{sa}, V^{sb}, V^{sc} is considered as three-phase supply voltages [26]. Based on phase neutral voltages and load currents, the actual and unconsidered powers of instantaneous values are computed. In the shunt active filter, the real and reactive power is computed created using (20).

$$\begin{bmatrix} P \\ Q \end{bmatrix} = \begin{bmatrix} V^{s\alpha} & V^{s\beta} \\ -V^{s\beta} & V^{s\alpha} \end{bmatrix} \begin{bmatrix} I^{l\alpha} \\ I^{l\beta} \end{bmatrix} \tag{20}$$

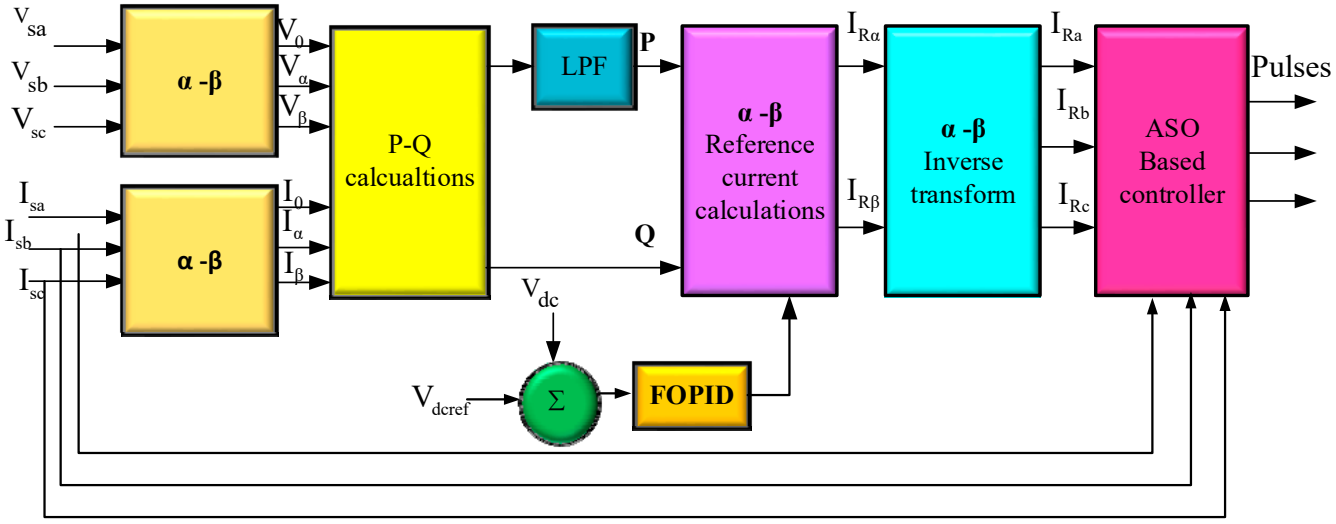

Figure 6. Block diagram of Shunt APF.

After that, the reference currents are computed based on Equation (21)

$$\begin{bmatrix} I^{Ra} \\ I^{Rb} \\ I^{Rc} \end{bmatrix} = \sqrt{\frac{2}{3}} \begin{bmatrix} 1 & 0 \\ -\frac{1}{2} & \frac{\sqrt{3}}{2} \\ -\frac{1}{2} & -\frac{\sqrt{3}}{2} \end{bmatrix} \begin{bmatrix} I^{R\alpha} \\ I^{R\beta} \end{bmatrix} \tag{21}$$

where I^{Ra}, I^{Rb}, I^{Rc} is represented as the current reference of the shunt active power filter. Based on the reference current, the error current is computed which must be compensated with the FOPID controller with the ASO algorithm [27]. In the shunt active power filter, the optimal pulses are selected and created on the error values of the system. The optimal pulses are generated with the help of the ASO algorithm. The detailed description of the FOPID controller with ASO optimization is presented in the following sections.

4.3. FOPID Controller

The proposed FOPID with the utilization of the ASO optimization technique is used to mitigate the PQ issues created in the HRES interface grid connected system which are due to voltage and current disruptions. Apart from convention controllers like Proportional Integral Derivative (PID) controller, Proportional Integral (PI), the FOPID controller provides the best gain values as it has five parameters. The error in voltage and current was reduced by the FOPID controller whose gain parameters were obtained with the use of the ASO technique. ASO is proposed to generate the optimal pulses to FOPID to reduce the error values in voltages and currents. UPQC-PQ device having a series controller and shunt controller whose control process is done with the FOPID controller to improve HRES system performance by reducing PQ issues [28]. The FOPID controller can be used to minimize error voltage and current by reducing error signals, eliminating signal undershoot and overshoot problems, and increasing the controller's speed of response, all of which are critical factors in achieving the maximum output to regulate the HRES system. The FOPID

controller speeds up the device, simplifies iso-damping, and is more resistant to parameter adjustments [29].

$$G(s) = \frac{u(s)}{e(s)} = K_P + \frac{K_i}{s^{\lambda}} + K_d s^{\mu} (\lambda, \mu \geq 0) \quad (22)$$

where $G(s)$ represents the FOPID controller's transfer function in the HRES system, $u(s)$ represents controller output, and $e(s)$ represents the HRES system's error signal [30–33]. Figure 7 illustrates the interface framework of a FOPID controller.

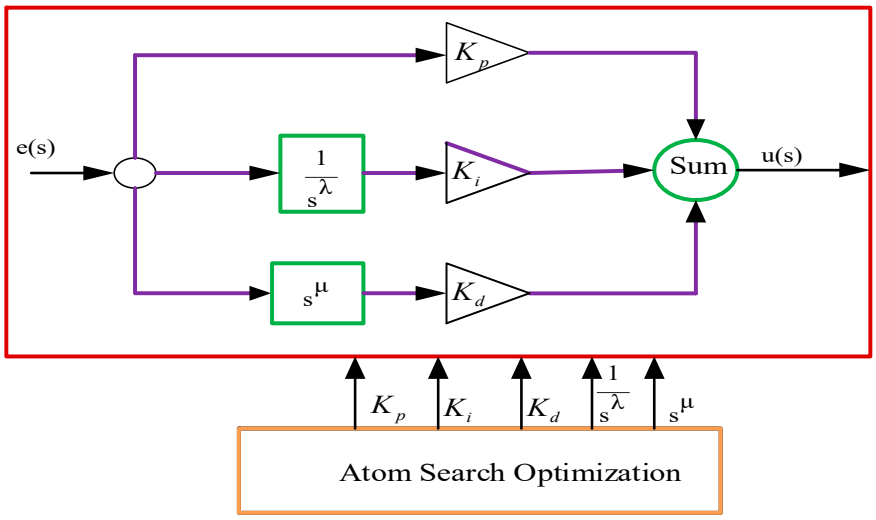

Figure 7. Control structure of FOPID.

Mathematical modelling of FOPID controller can be written as (23),

$$u(s) = K_P + K_i s^{-\lambda} e(s) + K_d s^{\mu} e(s) \quad (23)$$

K_P stands for proportional parameters, K_i for integral parameters, K_d for derivative parameters, $s^{-\lambda}$, s^{μ} for fractional order parameters, and $e(s)$ for error signal calculated from series and shunt active power filters. The error is calculated under differential load by comparing with reference and actual parameters. ASO techniques are used to generate the best optimal pulses required for the FOPID. The PQ issues in the HRES system are reduced with the following proposed controller. The detailed description of ASO is explained in the following section.

5. Atom Search Algorithm

The introduction of a new kind of meta-heuristic global optimization technique based on atom dynamics. Atom Search Optimization (ASO) is a population-based iterative heuristic global optimization method that may be used to solve a wide range of optimization issues. The ASO method mathematically simulates and replicates the atomic motion model seen in nature, in which atoms interact with one another through interaction forces arising from the Lennard-Jones potential and constraint forces coming from the bond-length potential.

5.1. Steps Followed in Control Strategy with ASO

In this section, the proposed ASO was stimulated by molecular dynamics. In the search space, the location of every atom describes the clarification and its calculation is based on the mass and gives the best solution. With the ASO technique shown in Figure 8, the gain parameters of the FOPID are selected based upon the minimizing of error of voltage and current. The fitness function of the proposed controller of ASO is presented as follows,

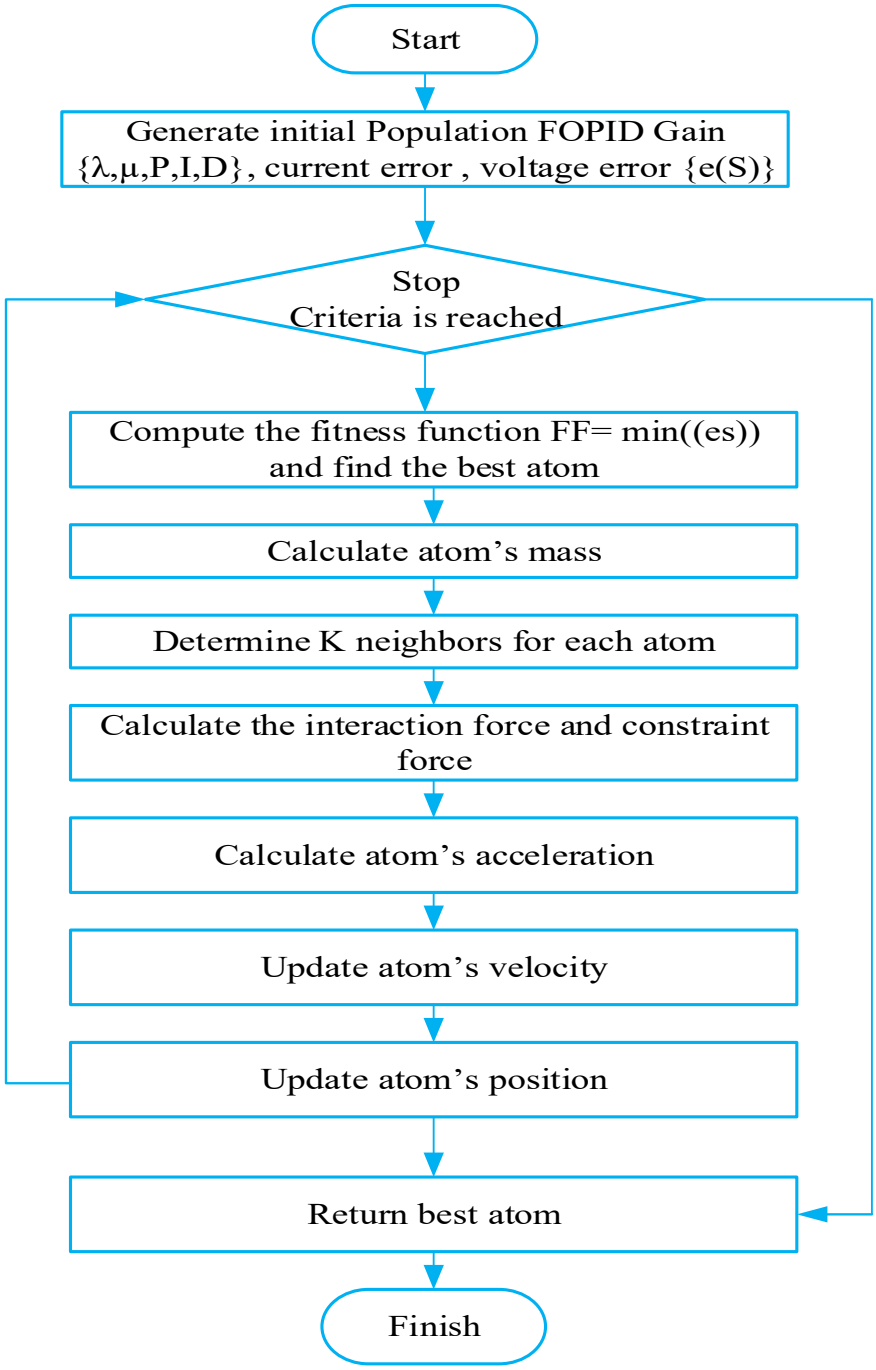

Figure 8. Flow chart of ASO technique.

5.1.1. Step 1: Initialization

ASO continues the streamlining process by making a vast number of random arrangements. Per loop, the particles change their speeds and locations, as well as the position of the best atom, which is also refreshed. Furthermore, particle acceleration is split into two parts. The most basic is the collaboration force, which is defined by the L-j potential, which is usually the vector sum of aversion and fascination from various particles.It is faced with the potential of bond length with and particle as well as the best particle is weighted location differentiation due to the necessary power. The computation satisfies the broken paradigm, and it can be carried out logically. The best atoms location and fitness are reverted, and the global optimum is expected.

5.1.2. Step 2: Fitness Evaluation

The fitness function is used to determine the best benefit parameters depending on the objective functions. In the equation, the fitness function is stated (24)

$$M^a(T) = e^{\frac{-Fit^a(T) - Fit^a(T)}{Fit^a_{worst}(T)}} \tag{24}$$

5.1.3. Step 3: Compute the Mass and C Neighbours

To compute the simplest level of the fitness function. The mass of its atom can be computed as (25),

$$m^a(T) = \frac{M^a(T)}{\sum_{n=1}^{N} M^b(T)} \tag{25}$$

where, $Fit^a{}_{best}(T)$ are the minimum fitness value and $Fit^a{}_{worst}(T)$ can be described as the maximum fitness value at the Tth iteration. $Fit^a(T)$ Can be represented as the fitness function value of the Tth iteration of the ith atom. The C neighbours can be computed based on the Equation (26), where a, b are the atoms.

$$C(T) = N - (N-2) \times \sqrt{\frac{T}{t}} \tag{26}$$

The discovery process of the ASA algorithm, the apiece, and each atom all need a large number of atoms with the best fitness parameters of the k neighbours. Atoms were expected to interrelate across as certain atoms with fitness parameters as it C neighbours to boost exploitations in the final step of iterations. Equation (26) can be used to calculate the C neighbours, T is maximum iterations, t dimension in time and N size of the population.

5.1.4. Step 4: Interaction Force and Acceleration Computation

The properties of atomic contact force and acceleration can be measured, and several components of random weight applied to the ith atom from the various atoms of force can be expressed as follows (27):

$$F^D_a(T) = \sum_{bebest}^{n} random_b f^D_{ab}(T) \tag{27}$$

where random is a random number in the range [0, 1], f fitness function. The acceleration can be calculated using the Equation (28).

$$G^D_a(T) = \alpha(T)(X^D_{best}(T) - X^D_a(T)) \tag{28}$$

The Lagrangian multiplier can be defined as the Equation (29),

$$\alpha(T) = \beta e^{-\frac{20T}{t}} \tag{29}$$

where β can be defined as the multiplier weight.

5.1.5. Step 5: The Updating Process

In this process, the velocity, as well as position, is ith atom at the condition of (t+1)th iteration can be denoted as (30) and (31)

$$V^D_a(t+1) = rand^D_a V^D_a(T) + A^D_a(t) \tag{30}$$

$$X^D_a(t+1) = X^D_a(t) + V^D_a(t+1) \tag{31}$$

The best strategy for achieving the exercise function and minimizing power quality problems can be selected following the upgrading process. The fitness functions can be used to choose the benefit parameters of the FOPID controller. The final condition

should be verified before using the optimal solutions that are maximal iteration obtained and constraints are evaluated. The optimal solutions are used to determine the optimal power flow of the HRES system. They can be achieved using the power quality reduction approach in the ASA algorithm. The proposed approach's efficiency metrics are explored in detail in the section below

6. Results and Discussion

This section validates and analyses the proposed method's efficiency. The suggested solution is designed to address power quality problems in HRES that are related to the grid. The key goal is to increase the system's reliability by addressing power quality problems. Established strategies have drawbacks, which are discussed in Section 3. As a result, the proposed controller and UPQC-PQ help to increase the system's power efficiency. Using UPQC-PQ with the proposed controller, the proposed system would provide improved reliability and voltage with current regulation in grid-connected HRES. ASO based FOPID controller is used to minimizing the PQ problems in the HRES system with the proposed UPQC-PQ device. The parameters are tested both with and without the system's PQ problems. The proposed methodology is run in MATLAB/Simulink with an Intel(R) Core(TM) i5-3570S CPU operating at 3.10 GHz, and the effects are evaluated. The proposed technique is compared to current PI controller-based GSA, BBO, ESA, RFA, and ASO techniques. Table 2 shows the parameters of the implementation. PQ problems like sag, swell, voltage disturbance, and harmonics in the system are created and validated. The problems of PQ is rewarded with the help of the UPQC-PQ device and an accurate proposed shunt as well as the series active power filter controller. The projected controller optimally controls the PQ issues by providing optimal pulses of series and shunt active power filter with help of the FOPID controller with ASO.The UPQC-PQ can provide the required power to solve the PQ issues and compensate for load demand in the system. In the UPQC-PQ design, the dc-link capacitor is used to provide essential power to alleviate PQ problems in the proposed HRES system. The PV and WT systems can be produced the power to encounter the load demand which is considered as the main source of the system. The WT and PV may be affected due to environmental conditions, which are solved by introducing the MPPT technique in the system. In the UPQC-PQ system, the generated power utilizes to compensate for the load demand and moderate issue of the PQ system. The UPQC-PQ system is linked with a grid-connected load system. The assessment of the proposed design configuration with three fault conditions in the system, such as sag, swell, voltage interference, and harmonics levels of signals. The device output is analyzed with various scenarios, which are described below.

Table 2. Simulation results summary for mode 1 and mode 2 operations.

THD	Phase	Mode 1				Mode 2			
		t_1	t_2	t_3	t_4	t_1	t_2	t_3	t_4
THD of V_s (%)	a	21.98	21.78	20.05	20.64	21.98	20.32	20.05	20.01
	b	18.08	16.86	14.41	14.91	18.08	14.40	18.40	17.4
	c	25.01	25.06	23.54	23.95	25.01	23.27	23.54	23.54
THD of I_L (%)	a	17.12	17.96	18.99	18.98	17.12	19.12	17.99	18.99
	b	26.82	25.17	27.21	27.18	26.82	27.02	26.21	27.21
	c	18.23	16.32	16.32	16.32	18.23	26.32	16.32	16.32
THD of I_s (%)	a	25.12	20.92	20.92	20.92	25.12	20.92	20.92	20.92
	b	27.31	12.33	12.32	12.32	27.31	25.32	26.32	12.32
	c	24.31	19.33	17.33	16.33	24.31	17.33	18.33	18.33

Mode I. *Power Quality improvement with P_{RES} Power injection ($P_{Res} > 0$).*

The proposed HRES system supplies power to the PCC in this mode of operation. To improve the PQ at PCC the inverter which is the interface to the grid is used to transfer the power from RES to the PCC. A non-linear load generally uncontrolled diode rectifier with series RL is connected at PCC. Real and reactive power to the local load is being supplied by the RES and the excess real power is transferred to the grid. The THD of 21.98% is produced by adding the 5th harmonic voltage source since grid voltage is taken as non-sinusoidal. Figure 9a,b shows the active powers P_{DG}, P_{load}, P_{grid} and reactive powers Q_{DG}, Q_{load}, Q_{grid}. The dynamic performance is studied in case I and case II. THD's are presented during this case in Table 2. Figure 10 depicts PV irradiance, wind speed and DG power.

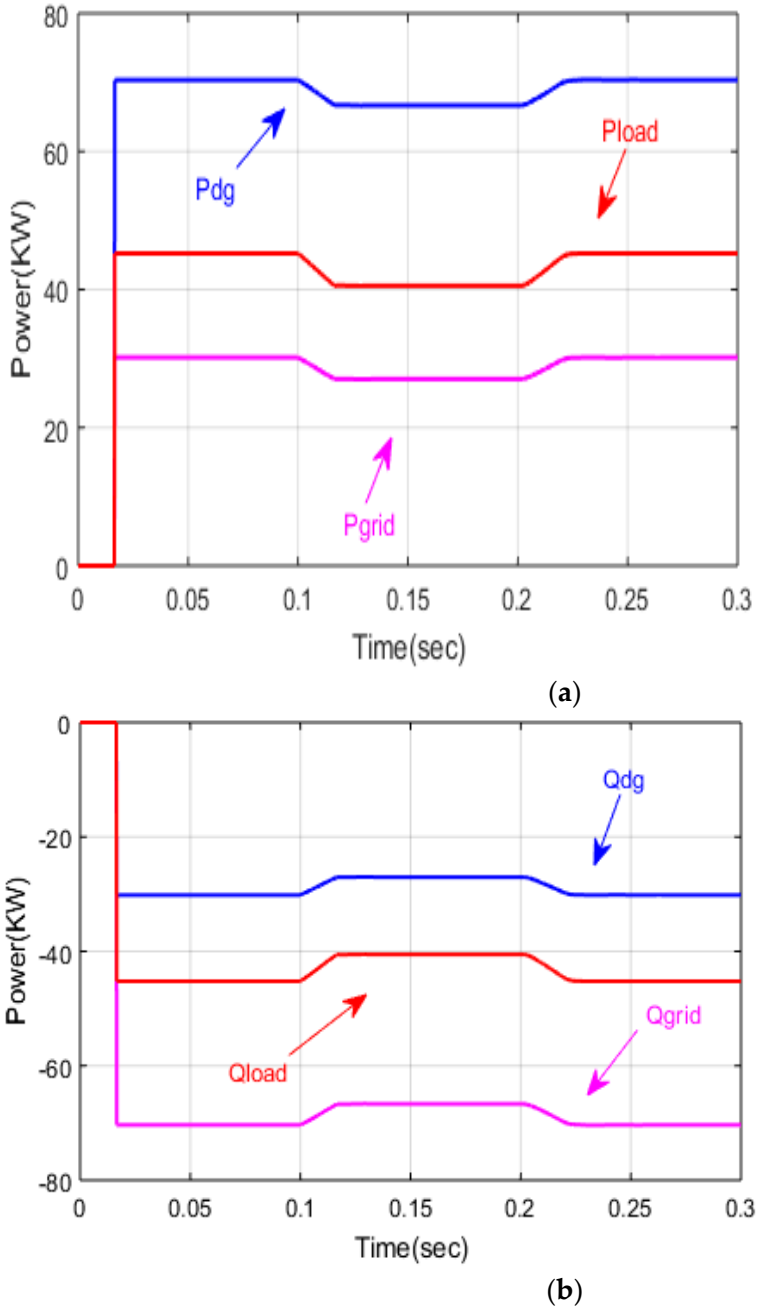

Figure 9. (**a**) Active Power, (**b**) Reactive power.

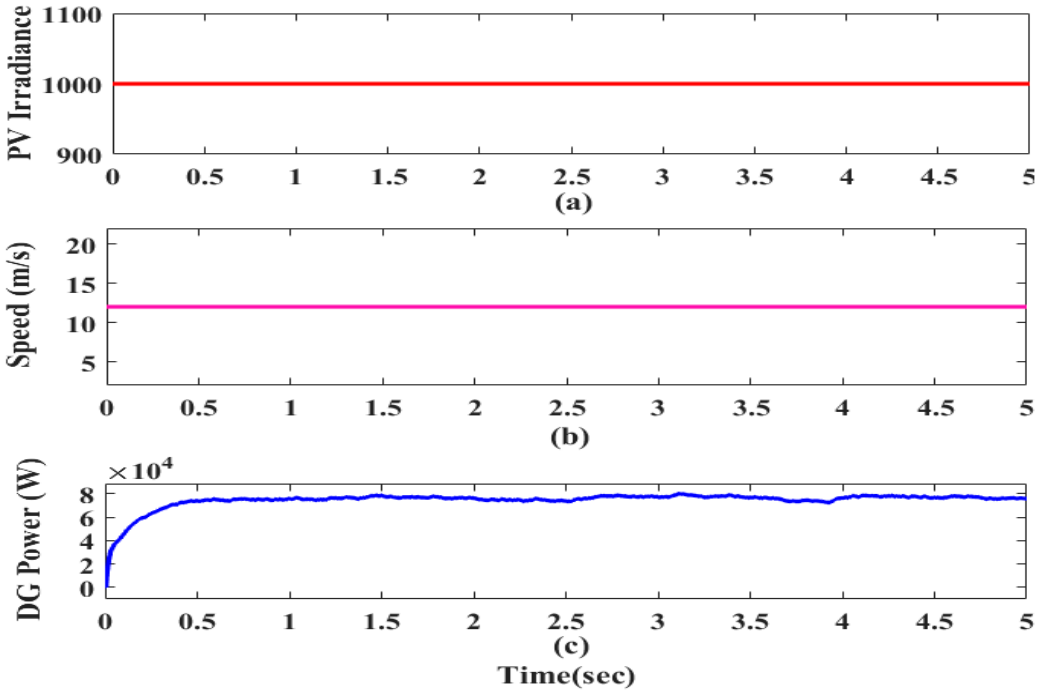

Figure 10. (**a**) Irradiance (**b**) Wind speed (**c**) DG Power.

Mode II. *Power Quality improvement (P_{Res} = 0).*

Here inverter which is a grid interface is acting like Shunt APF. In this case, the inverter consumes a very little amount of real power from the grid to reduce the losses and maintain DC link voltage. The inverter provides the load reactive and harmonic power. Figure 11a,b shows the active powers P_{DG}, P_{load}, P_{grid} and reactive powers Q_{DG}, Q_{load}, Q_{grid}. The total reactive power is supplied by the inverter and active power is supplied by the grid. The dynamic performance is studied in case I and case II.

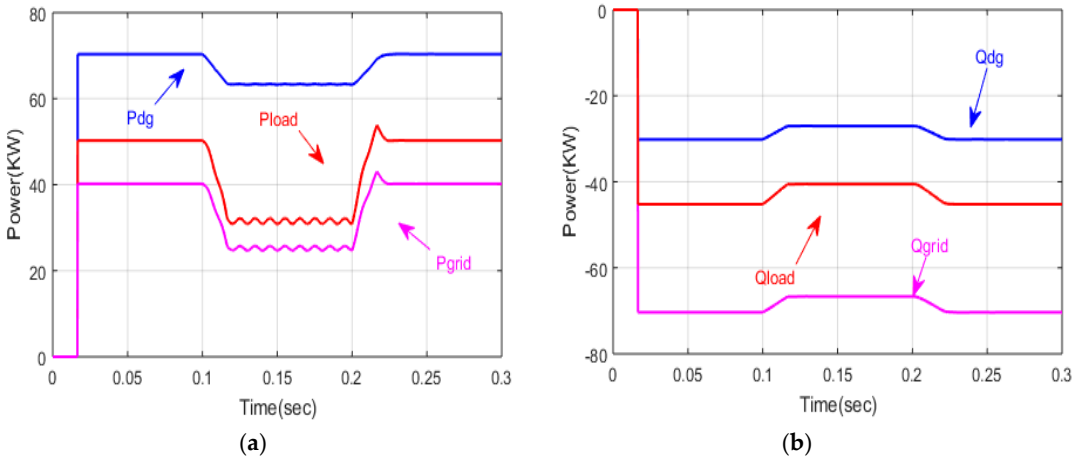

Figure 11. (**a**) Active Power, (**b**) Reactive power.

Case I: Condition for Nonlinear Load variation
Case II: Condition for Unbalance Non-Linear Load
Case III: Condition for Voltage and current sag
Case IV: Condition for Voltage and current swell
Case V: Condition for Voltage and current disturbances

The five cases are individually analyzed with the design parameters of voltage, current, power, and injected power from the UPQC-PQ.

6.1. Case I: Condition for Non-Linear Load Variation

To study the dynamic performance of the non-linear loads this is time-varying in nature by introducing a nonlinear load variation. Here a non-linear load is considered to be a diode rectifier with R-L load. An addition of another R-L load is being added to the existing load at t = 0.1 s and removed at 0.22 s. Thus the load current is increased from 55 A to 62.2 A. The dynamic performance of the PCC voltage V_s, supply current I_s, load current I_L and compensating currents I_C are shown in Figure 12. The THD of the grid current is reduced from 25.15% before compensation to 20.92% after compensation with load current THD of 18.99% and 18.98% due to voltage disruption due to an increase in PCC current.

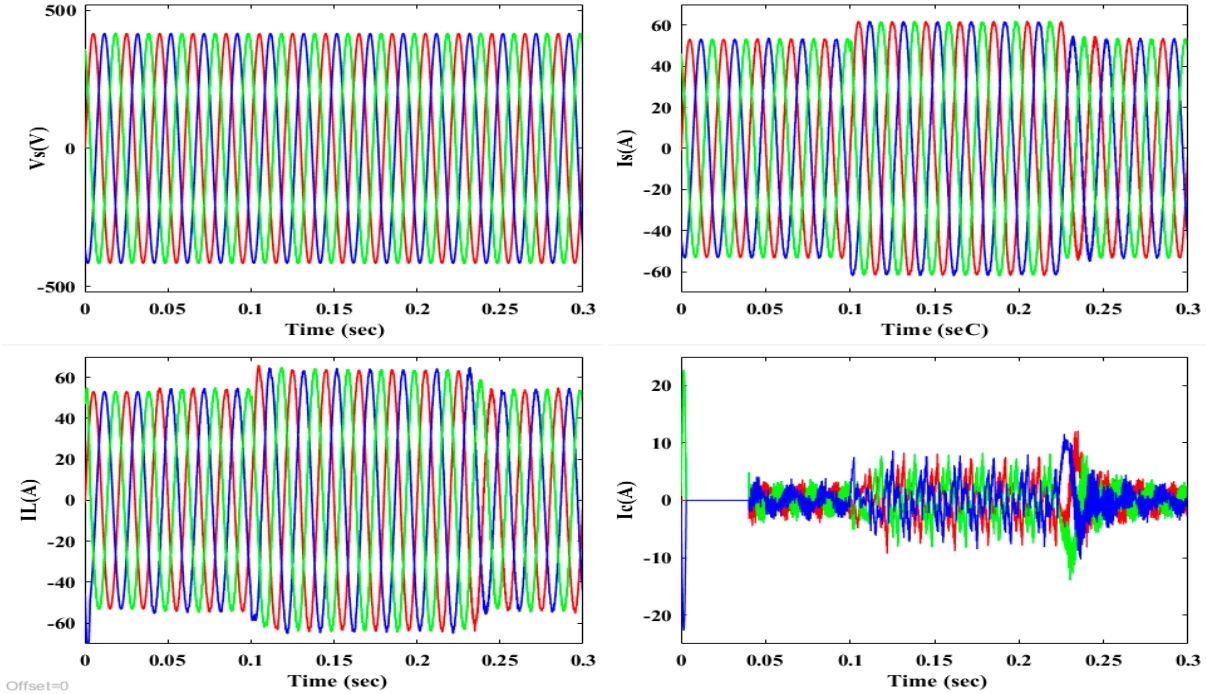

Figure 12. PCC voltage V(s), Grid current (Is), Load current (I_L), Inverter Terminal out current I(c).

6.2. Case II: Condition for Unbalanced Nonlinear Load

An unbalanced load is being connected at the PCC which initially consists of a diode rectifier with an R-L load. To this system, a single-phase R-L load is connected between any two phases during t = 0.1 s to 0.22 s. From Figure 13 we can observe that PCC voltage, supply current, load current, inverter output currents are balanced even under unbalance loads connected at the PCC. For phase a, b and c the TDS of the load current are 18.98%, 27.18% and 16.32% and grid currents are 20.92%, 12.32% and 16.33% during t = 0.1 s to 0.22 s. The system can be balanced by compensating harmonic and reactive load current components.

6.3. Case III: Voltage and Current Sag Condition

In this state, the sag is created in the HRES system by creating a fault. The voltage and current sag must be resolved to provide a linear and stable operation of the system. The UPQC-PQ is used to provide the required power to satisfy load demand by mitigating PQ problems. In Figure 14, the injected voltage, compensated voltage, and voltage sag. As seen in Figure 15, sag current is compensated current and injected current with the UPQC-PQ device. Figure 16 shows the total harmonics distortion of the proposed method and comparison with the existing methods. The injected voltage and current from the

proposed controller is used to compensate for the PQ issues. In UPQC-PQ both series and shunt APF's balance the voltage and current. In this case study, the swell conditions at voltage signals are investigated.

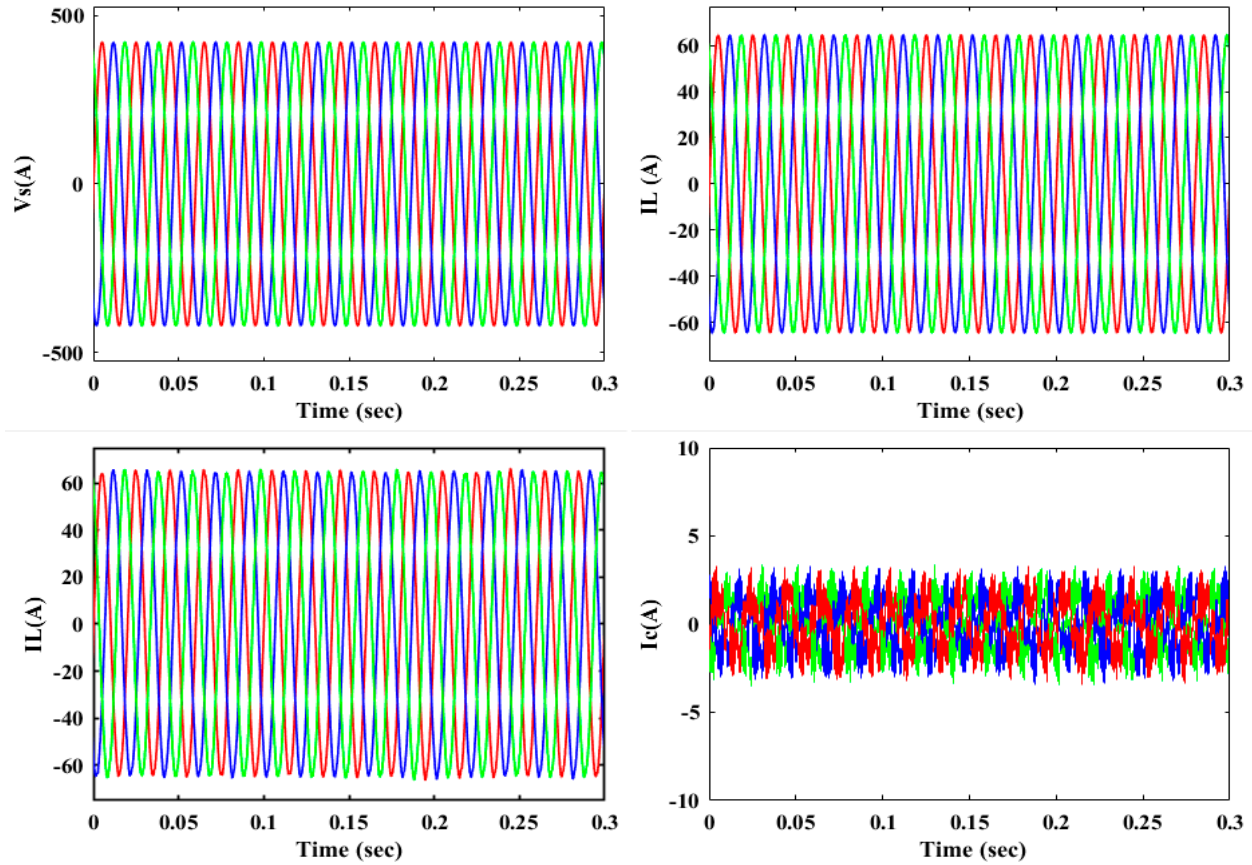

Figure 13. PCC voltage V(s), Grid current (Is), Load current (I_L), Inverter Terminal out current I(c).

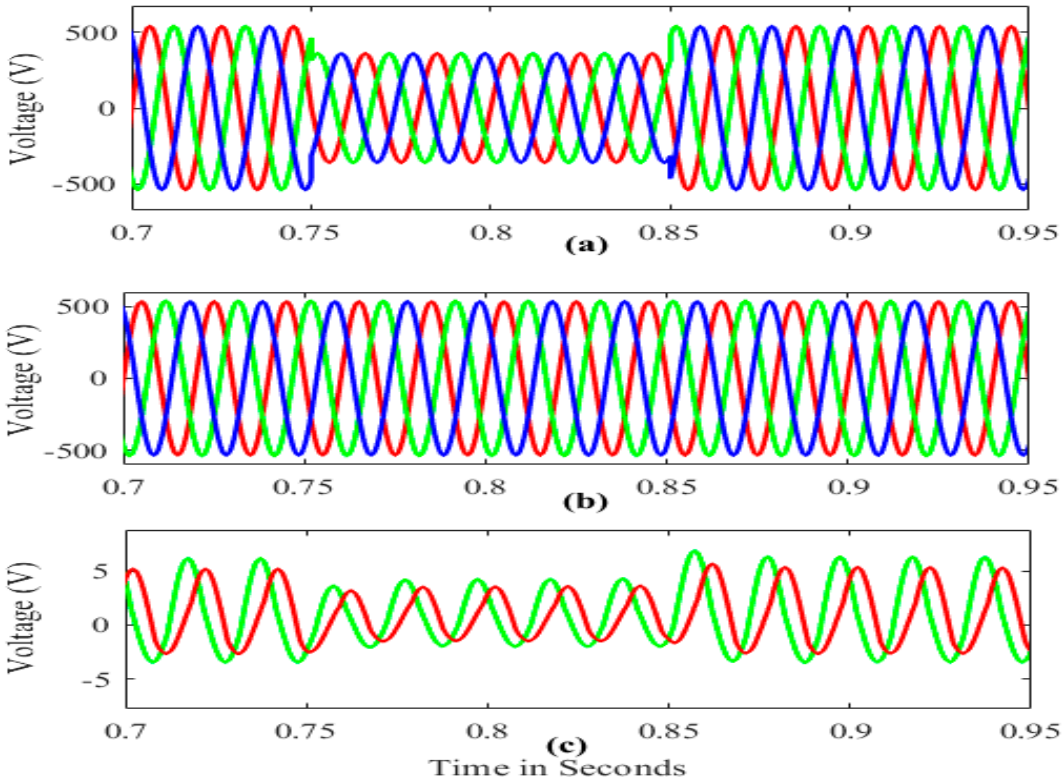

Figure 14. Voltage Sag Condition (**a**) Source Voltage (**b**) Load Voltage (**c**) Injected Voltage.

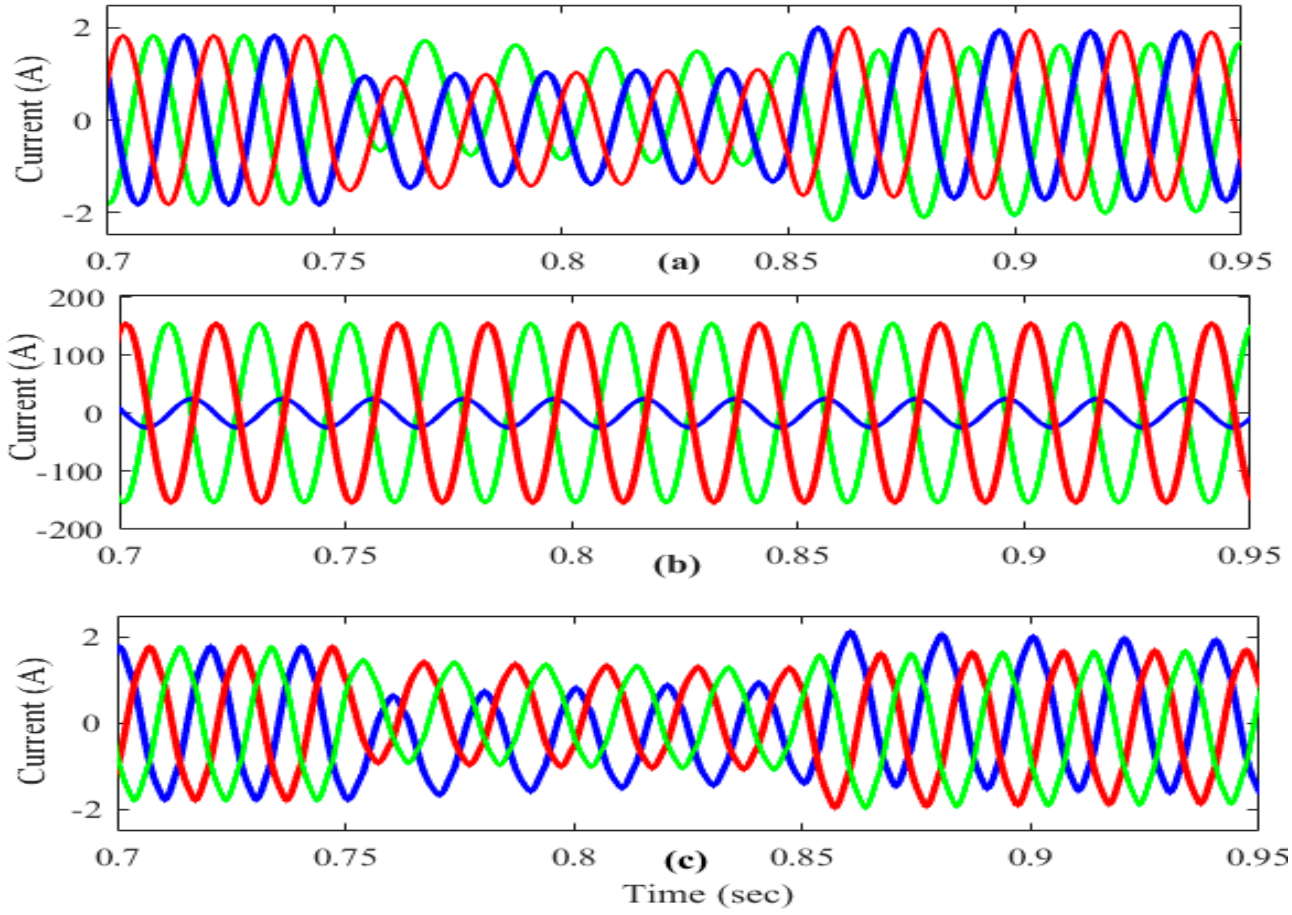

Figure 15. Current Sag Condition (**a**) Source current (**b**) Load current (**c**) Injected current.

6.4. Case IV: Voltage and Current Swell Condition

Increased voltage and current is generally termed as swell when compared with the reference voltage and current. The condition for swell is observed due to the faults created in the system. The swell must be resolved to increase the system's stability. A voltage swell of magnitude 520 V has been observed and being compensated with the UPQC-PQ device during t = 0.75 s to 0.85 s illustrated in Figure 17. Similarly, Figure 18, depicts the condition for current swell during t = 0.75 s to 0.85 s whose magnitude is being increased During this condition the dc-link capacitor is used to meet the load demand and mitigate the PQ problems with ASO based FOPID controllers which is primarily used to determine the error values that can be corrected by choosing optimum values.

6.5. Case V: Voltage Disturbances Condition

Normally the disturbances in voltage and current are usually occurred due to the nonlinear, unbalance, or critical loads at the load side. PQ problems related under such conditions are mitigated in the HRES grid connected system UPQC-PQ device consisting of two modes of operation like series APF and shunt APF is used to compensate the problems related to voltage and current disruption. The optimal pulses are received by the ASO technique which is fed to the FOPID controller which moderately operates the series APF and shunt APF to mitigate the voltage and current-related disturbances and maintain the system stable and reliable. Figures 19 and 20 shows the condition for voltage and current disturbances.

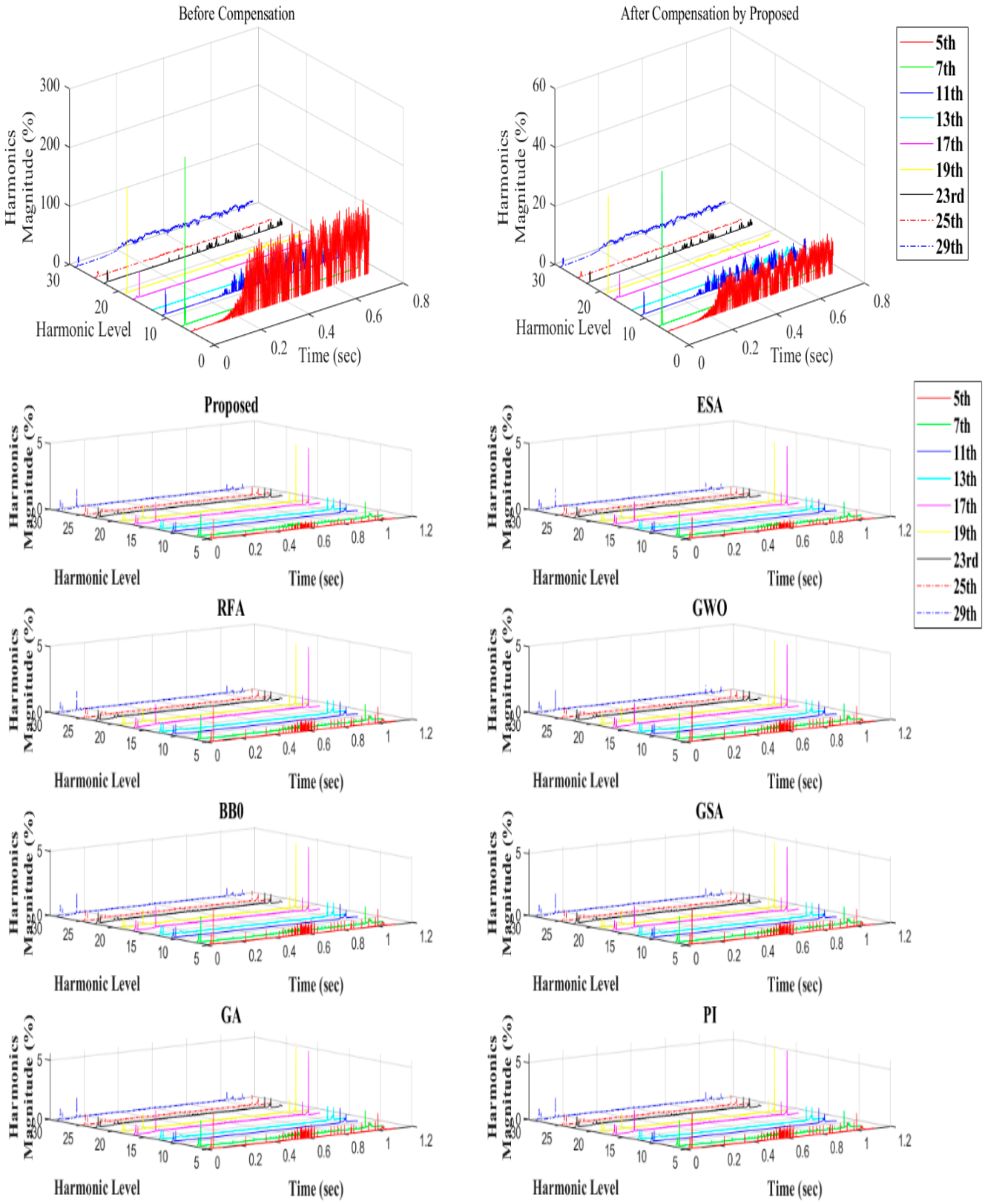

Figure 16. Analysis of THD comparison.

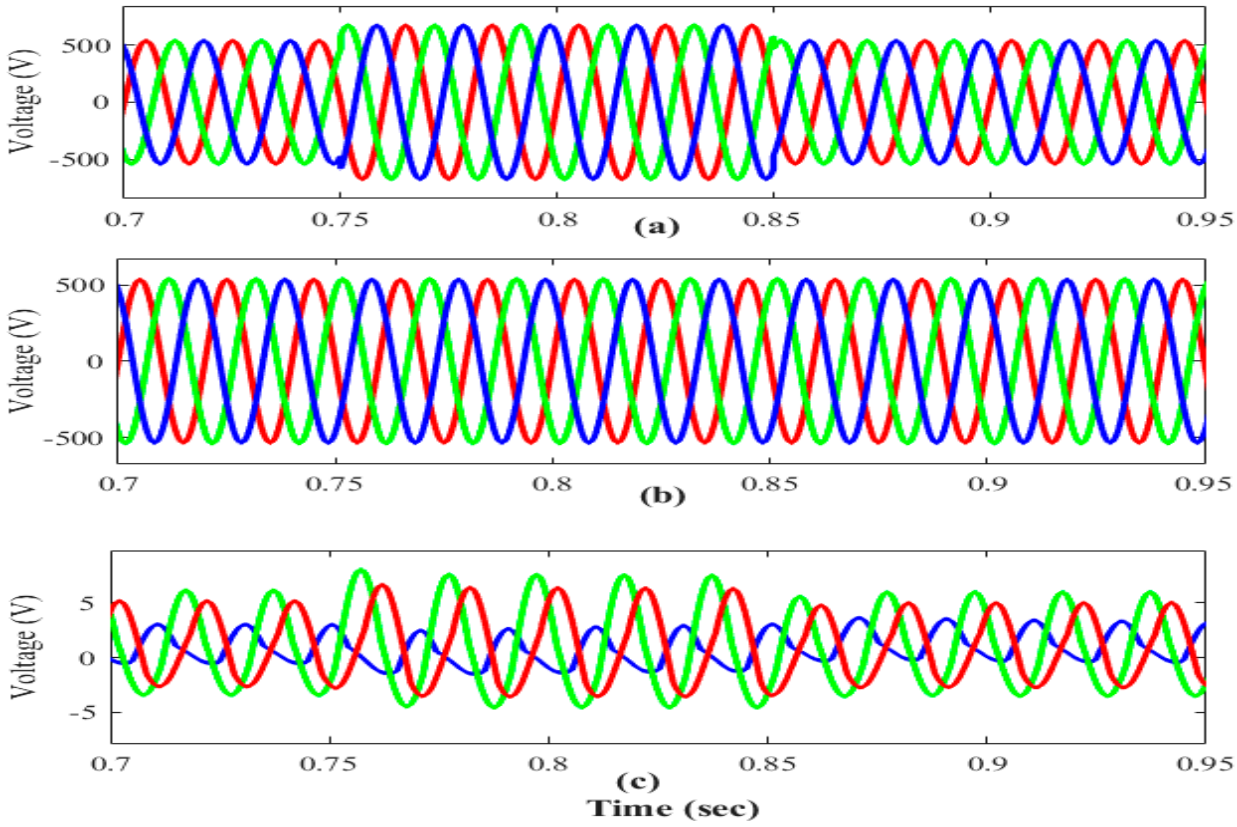

Figure 17. Analysis of voltage swell conditions (**a**) Source Voltage (**b**) Load Voltage (**c**) Injected Voltage.

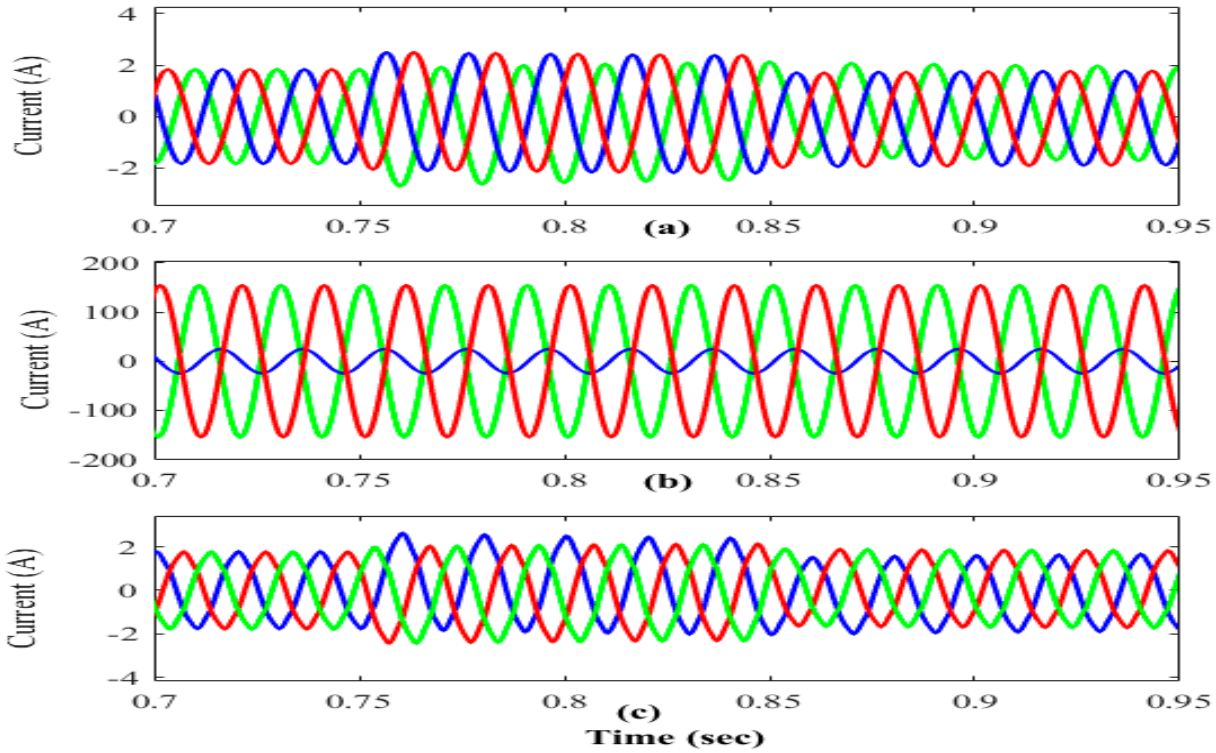

Figure 18. Analysis of current swell conditions (**a**) Source Current (**b**) Load Current (**c**) Injected Current.

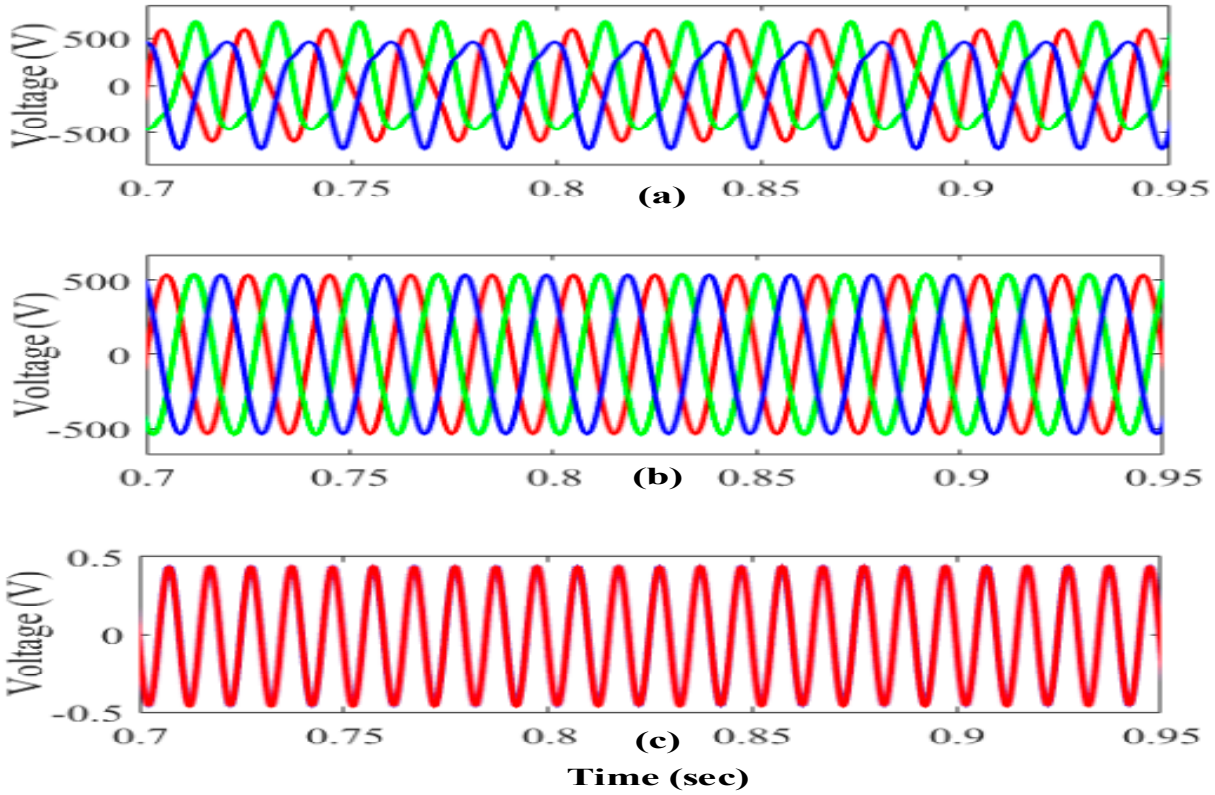

Figure 19. Analysis of voltage disturbance conditions (**a**) Source Voltage (**b**) Load Voltage (**c**) Injected Voltage.

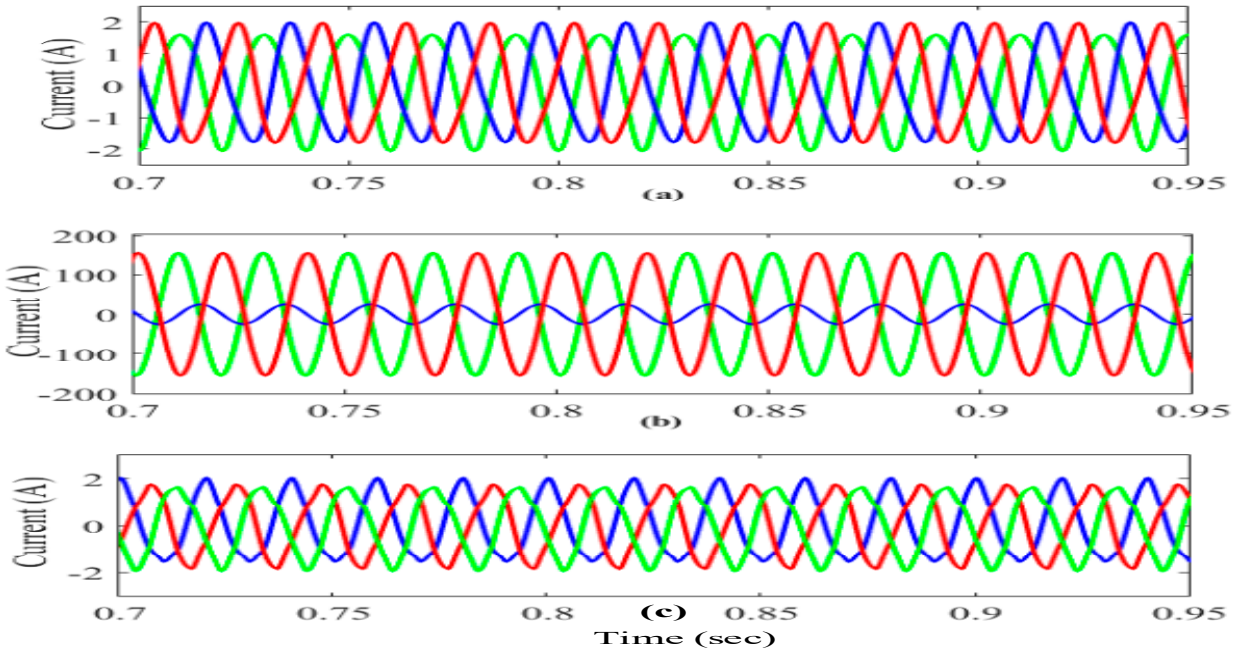

Figure 20. Analysis of current-voltage disturbance conditions (**a**) Source Current (**b**) Load Current (**c**) Injected current.

6.6. Comparison Analysis

The ASO-based FOPID controller in HRES interfaced grid connected system is analyzed under nonlinear load, unbalanced load, sag, swell, interruptions and harmonics reduction. Figures 21 and 22 shows the real and reactive power with the proposed controlling technique which gives the best results when compared with the existing techniques like

PI, GA, GSA, BBO, GWO, RFA and ESA. The total harmonic reduction was also achieved to the best level and maintained within the IEEE519 standards and the values are presented in Table 3. According to the results of the study, the proposed controller has the best real and reactive power output. Similarly, with the proposed FOPID controller, grid side power was kept stable. Figure 20 illustrates how effectively in the HRES generation system the grid power is compensated with a storage system under varying environmental conditions. The FOPID controller with ASO is configured to keep the grid side power stable and reduce the harmonics to a lower percentage which falls under IEEE 519 standards. The proposed controller achieves the best results by maintaining the system stable and reliable. ASO based FOPID controller in the HRES interfaced grid-connected system with the use of UPQC-PQ which is effectively mitigating the PQ problems related to nonlinear load, unbalanced loads, sag, swell and interruptions by generating the optimal pulses for series APF and shunt APF.

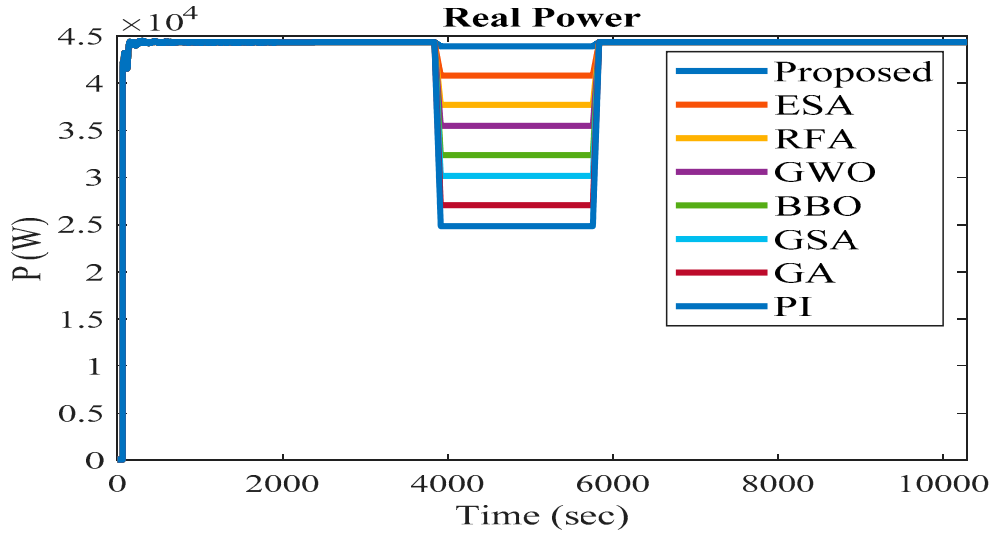

Figure 21. Real power comparison.

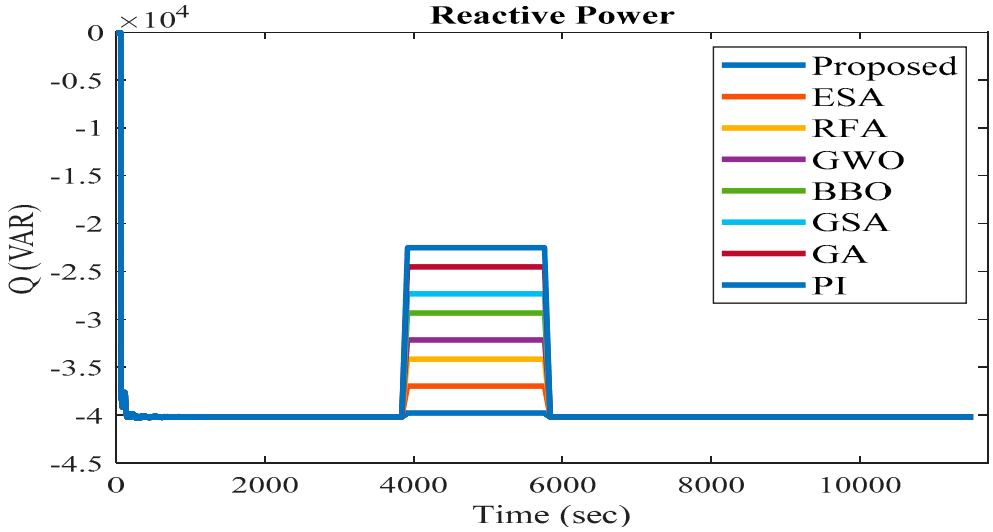

Figure 22. Reactive power comparison.

Table 3. THD comparison before and after UPQC.

S.No	Methods	Before UPQC-PQ								
		5	**7**	**11**	**13**	**17**	**19**	**23**	**25**	**29**
1	Proposed	22.42	11.55	11.21	10.12	10.09	10.25	10.18	10.09	10.05
2	ESA	37.37	11.65	11.3	10.45	10.36	10.29	10.22	10.16	10.11
3	RFA	36.32	11.45	11.2	10.4	10.34	10.25	10.2	10.13	10.09
4	GWO	35.55	11.41	11.19	10.3	10.32	10.2	10.19	10.11	10.07
5	BBO	34.65	11.35	10.48	10.2	10.28	10.19	10.17	10.1	10.06
6	GSA	33.71	11.3	10.42	10.19	10.18	10.15	10.14	10.09	10.05
7	GA	32.32	11.25	10.31	10.18	10.15	10.13	10.11	10.07	10.04
8	PI	31.37	11.2	10.22	10.14	10.13	10.11	10.09	10.05	10.03
S.No	**Methods**	**After UPQC-PQ**								
		5	**7**	**11**	**13**	**17**	**19**	**23**	**25**	**29**
1	Proposed	1.16	0.25	0.22	0.21	0.19	0.15	0.1	0.09	0.08
2	ESA	3.73	0.3	0.28	0.25	0.2	0.19	0.15	0.14	0.13
3	RFA	3.65	0.29	0.25	0.23	0.18	0.17	0.13	0.12	0.11
4	GWO	3.42	0.28	0.23	0.2	0.16	0.15	0.1	0.09	0.08
5	BBO	3.4	0.27	0.22	0.19	0.14	0.13	0.08	0.07	0.06
6	GSA	3.35	0.25	0.2	0.15	0.12	0.11	0.07	0.06	0.05
7	GA	3.21	0.2	0.19	0.13	0.1	0.09	0.06	0.04	0.03
8	PI	3.1	0.18	0.17	0.12	0.09	0.05	0.04	0.03	0.02

7. Conclusions

Power quality improvement in the HRES Grid connected system has become a promising research area. With the use of non-linear loads, unbalanced loads and high-frequency switching characteristics PQ problems occur on the load side. To overcome PQ problems we need to adopt custom power devices which are playing a vital role to mitigate such issues.

- In the proposed paper UPQC-PQ device which is controlled with ASO based FOPID controller is proposed.
- The optimal gains required to operate the FOPID controller of UPQC-PQ is produced with the use of the ASO technique.
- In the proposed system various analyses have been observed such as Mode I: Power Quality improvement with P_{RES} Power injection. ($P_{Res} > 0$),Mode II: Power Quality improvement ($P_{Res} = 0$) and THD reduction.
- In addition, we have addressed PQ issues such as sag, swell and disturbance conditions for both voltage/current related problems
- The proposed system is validated in the MATLAB/Simulink platform. The proposed method produces the best results when compared with various existing methods like PI, GA, GSA, GWO, BBO, RFA and ESA.

Future Work: The future work can be carried out with various new controlling strategies which can be operated by implementing Hybrid Algorithms whose performance characteristics can be improved in terms of efficiency, speed of the response etc.

Author Contributions: Conceptualization C.R.R., B.S.G. and G.S.R.; methodology, C.R.R., B.S.G. and F.A.; software, B.S.G.; validation, C.R.R., B.S.G. and G.S.R.; formal analysis, E.C.B.; investigation, C.R.R., B.S.G. and G.S.R.; resources, C.R.R., B.S.G. and F.A.; data curation, G.S.R., F.A. and E.C.B.; writing—original draft preparation, B.S.G.; writing—review and editing, C.R.R., B.S.G. and G.S.R.; visualization, F.A. and E.C.B.; supervision, G.S.R. and F.A.; project administration, G.S.R. and

F.A.; funding acquisition E.C.B. All authors have read and agreed to the published version of the manuscript.

Funding: This research received no external funding.

Institutional Review Board Statement: Not applicable.

Informed Consent Statement: Not applicable.

Data Availability Statement: Not applicable.

Conflicts of Interest: The authors declare no conflict of interest.

Abbreviations

HRES	Hybrid Renewable Energy Sources
UPQC-PQ	Unified Power Quality Conditioner with Real and Reactive power
FOPID	Functional Order Proportional Integral Derivative
THD	Total Harmonic Distortion
PI	Proportional Integral
GSA	Gravitational Search Algorithm
BBO	Biogeography Based Optimization
GWO	Grey Wolf Optimization
ESA	Extended Search Algorithm
RFA	Random Forest Algorithm
GA	Genetic Algorithm
PV	Photovoltaic
WT	Wind Turbine
BESS	Battery Energy Storage System
SSC	Synchronous Series Compensator
DVR	Dynamic Voltage Restoration
DSTATCOM	Distribution Static Compensator
TCR	Thyristor-Controlled Reactor
PCC	Point of Common Coupling
ANIFS	Adaptive Neuro-Fuzzy Interference System
MGWO	Modified Grey Wolf Optimization
ACT	Adaptive Control Technique
SVPWM	Space Vector Pulse Width Modulation
FLC	Fuzzy Logic controller
VSI	Voltage Source Inverters
LPF	Low pass filter
APF	Active Power Filter

References

1. Mira, M.C.; Zhang, Z.; Knott, A.; Andersen, M.A.E. Analysis, Design, Modeling, and Control of an Interleaved-Boost Full-Bridge Three-Port Converter for Hybrid Renewable Energy Systems. *IEEE Trans. Power Electron.* **2017**, *32*, 1138–1155. [CrossRef]
2. Qazi, A.; Hussain, F.; Rahim, N.A.; Hardaker, G.; Alghazzawi, D.; Shaban, K.; Haruna, K. Towards Sustainable Energy: A Systematic Review of Renewable Energy Sources, Technologies, and Public Opinions. *IEEE Access* **2019**, *7*, 63837–63851. [CrossRef]
3. Liang, X. Emerging Power Quality Challenges Due to Integration of Renewable Energy Sources. *IEEE Trans. Ind. Appl.* **2017**, *53*, 855–866. [CrossRef]
4. Goud, B.S.; Rao, B.L.; Reddy, B.N.; Rajesh, N.; Anjan, B.; Reddy, C.R. Optimization Techniques in PV-Wind based Distribution Generation—A Brief Review. In Proceedings of the 2020 IEEE 17th India Council International Conference (INDICON), New Delhi, India, 11–13 December 2020; pp. 1–6.
5. Kalla, U.K.; Kaushik, H.; Singh, B.; Kumar, S. Adaptive Control of Voltage Source Converter Based Scheme for Power Quality Improved Grid-Interactive Solar PV–Battery System. *IEEE Trans. Ind. Appl.* **2019**, *56*, 787–799. [CrossRef]
6. Shukl, P.; Singh, B. Delta-Bar-Delta Neural-Network-Based Control Approach for Power Quality Improvement of Solar-PV-Interfaced Distribution System. *IEEE Trans. Ind. Inform.* **2020**, *16*, 790–801. [CrossRef]
7. Elmetwaly, A.H.; Eldesouky, A.A.; Sallam, A.A. An Adaptive D-FACTS for Power Quality Enhancement in an Isolated Microgrid. *IEEE Access* **2020**, *8*, 57923–57942. [CrossRef]

8. Jain, S.K.; Soni, A. Lecture Notes in Electrical Engineering. In *Mitigation of Power Quality for Wind Energy Using Transmission Line Based on D-STATCOM*; Springer: Singapore, 2020; pp. 927–935.
9. Mallesham, G.; Kumar, C.H.S. Power Quality Improvement of Weak Hybrid PEMFC and SCIG Grid Using UPQC. In *Learning and Analytics in Intelligent Systems*; Springer: Cham, Switzerland, 2020; pp. 406–413.
10. Mehta, G.; Singh, S. Power quality improvement through grid integration of renewable energy sources. *IETE J. Res.* **2013**, *59*, 210. [CrossRef]
11. Mosobi, R.W.; Chichi, T.; Gao, S. Power quality analysis of hybrid renewable energy system. *Cogent Eng.* **2015**, *2*, 1005000. [CrossRef]
12. Karami, M.; Cuzner, R.M. A distributed controller for DC microgrids stability enhancement. In Proceedings of the 2016 IEEE International Conference on Renewable Energy Research and Applications (ICRERA), Birmingham, UK, 20–23 November 2016; pp. 556–561.
13. Patel, A.; Mathur, H.D.; Bhanot, S. An improved control method for unified power quality conditioner with unbalanced load. *Int. J. Electr. Power Energy Syst.* **2018**, *100*, 129–138. [CrossRef]
14. Dash, S.K.; Ray, P.K. Power Quality Improvement Utilizing PV Fed Unified Power Quality Conditioner Based on UV-PI and PR-R Controller. *CPSS Trans. Power Electron. Appl.* **2018**, *3*, 243–253. [CrossRef]
15. Ravinder, K.; Bansal, H.O. Investigations on shunt active power filter in a PV-wind-FC based hybrid renewable energy system to improve power quality using hardware-in-the-loop testing platform. *Electr. Power Syst. Res.* **2019**, *177*, 105957. [CrossRef]
16. Chishti, F.; Murshid, S.; Singh, B. Development of Wind and Solar Based AC Microgrid with Power Quality Improvement for Local Nonlinear Load Using MLMS. *IEEE Trans. Ind. Appl.* **2019**, *55*, 7134–7145. [CrossRef]
17. Hussain, J.; Hussain, M.; Raza, S.; Siddique, M. Power Quality Improvement of Grid Connected Wind Energy System Using DSTATCOM-BESS. *Int. J. Renew. Energy Res.* **2019**, *9*, 1388–1397.
18. Jin, T.; Chen, Y.; Guo, J.; Wang, M.; Mohamed, M.A. An effective compensation control strategy for power quality enhancement of unified power quality conditioner. *Energy Rep.* **2020**, *6*, 2167–2179. [CrossRef]
19. Krishna, D.; Sasikala, M.; Ganesh, V. Adaptive FLC-based UPQC in distribution power systems for power quality problems. *Int. J. Ambient. Energy* **2020**, 1–11. [CrossRef]
20. Hussain, M.M.; Siddique, M.; Raees, A.; Nouman, M.; Javed, W.; Razaq, A. Power Management through Smart Grids and Advance Metering Infrastructure. In Proceedings of the 2020 6th IEEE International Energy Conference (ENERGYCon), Gammarth, Tunisia, 28 September–1 October 2020; pp. 767–772.
21. Ahmad, R.F.; Siddique, M.; Riaz, K.; Hussain, M.M.; Bhatti, M. Blockchain based Secure Energy Trading Mechanism for Smart Grid. *Pak. J. Eng. Technol.* **2021**, *4*, 100–107. [CrossRef]
22. Razaq, A.; Hussain, M.; Javed, W.; Javed, T.; Memon, Z. Detection and Prevention of Denial-of-Service in Cloud-based Smart Grid. In Proceedings of the 10th International Conference on Smart Cities and Green ICT Systems, Prague, Czech Republic, 28–30 April 2021; Scitepress Digital Library: Setubal, Portugal, 2021; pp. 172–179.
23. Naidu, R.P.K.; Meikandasivam, S. Power quality enhancement in a grid-connected hybrid system with coordinated PQ theory & fractional order PID controller in DPFC. *Sustain. Energy Grids Netw.* **2020**, *21*, 100317. [CrossRef]
24. Bajaj, M.; Singh, A.K. An analytic hierarchy process-based novel approach for benchmarking the power quality performance of grid-integrated renewable energy systems. *Electr. Eng.* **2020**, *102*, 1153–1173. [CrossRef]
25. Bajaj, M.; Singh, A.K. Hosting capacity enhancement of renewable-based distributed generation in harmon-ically polluted distribution systems using passive harmonic filtering. *Sustain. Energy Technol. Assess.* **2021**, *44*, 101030.
26. Goud, B.S.; Rekha, R.; Jyostna, M.R.L.; Sarala, S.; Rao, B.L.; Reddy, C.R. Energy Management and Power Quality Improvement in HRES Grid-Connected System. In Proceedings of the 2020 FORTEI—International Conference on Electrical Engineering (FORTEI-ICEE), Bandung, Indonesia, 23–24 September 2020; pp. 174–178.
27. Devassy, S.; Singh, B. Design and Performance Analysis of Three-Phase Solar PV Integrated UPQC. *IEEE Trans. Ind. Appl.* **2018**, *54*, 73–81. [CrossRef]
28. Choudhury, S.; Dash, T.; Bhowmik, P.; Rout, P.K. A novel control approach based on hybrid Fuzzy Logic and Seeker Optimization for optimal energy management between micro-sources and supercapacitor in an islanded Microgrid. *J. King Saud Univ.-Eng. Sci.* **2018**, *32*, 27–41. [CrossRef]
29. Suresh, V.; Muralidhar, M.; Kiranmayi, R. Modelling and optimization of an off-grid hybrid renewable energy system for electrification in a rural areas. *Energy Rep.* **2020**, *6*, 594–604. [CrossRef]
30. Mayer, M.J.; Szilágyi, A.; Gróf, G. Environmental and economic multi-objective optimization of a household level hybrid renewable energy system by genetic algorithm. *Appl. Energy* **2020**, *269*, 115058. [CrossRef]
31. Bajaj, M.; Singh, A.K.; Alowaidi, M.; Sharma, N.K.; Sharma, S.K.; Mishra, S. Power Quality Assessment of Distorted Distribution Networks Incorporating Renewable Distributed Generation Systems Based on the Analytic Hierarchy Process. *IEEE Access* **2020**, *8*, 145713–145737. [CrossRef]
32. Goud, B.S.; Reddy, C.R. Essentials for Grid Integration of Hybrid Renewable Energy Systems: A Brief Review. *Int. J. Renew. Energy Res.* **2020**, *10*, 813–830.
33. Goud, B.S.; Rao, B.L. An intelligent technique for optimal power quality enhancement (OPQE) in a HRES grid connected system: ESA technique. *Int. J. Renew. Energy Res.* **2020**, *10*, 317–328.